REPUBLIC OF TURKEY

ADANA ALPARSLAN TÜRKEŞ SCIENCE AND TECHNOLOGY UNIVERSITY

GRADUATE SCHOOL OF NATURAL AND APPLIED SCIENCES

DEPARTMENT OF BIOENGINEERING

PREPARATION OF NEOPTERIN IMPRINTED NANOFILM COATED SURFACE PLASMON RESONANCE SENSORS FOR DETECTION OF NEOPTERIN FROM HUMAN SERUM

BURCU EREN YÜNGEVİŞ

MASTER OF SCIENCE

ADANA 2022

REPUBLIC OF TURKEY
ADANA ALPARSLAN TÜRKEŞ SCIENCE AND TECHNOLOGY UNIVERSITY

GRADUATE SCHOOL OF NATURAL AND APPLIED SCIENCES
DEPARTMENT OF BIOENGINEERING

PREPARATION OF NEOPTERIN IMPRINTED NANOFILM COATED SURFACE PLASMON RESONANCE SENSORS FOR DETECTION OF NEOPTERIN FROM HUMAN SERUM

BURCU EREN YÜNGEVİŞ
MASTER OF SCIENCE

SUPERVISOR
PROF. DR. GÖZDE BAYDEMİR PEŞİNT

ADANA, 2022

ABSTRACT

PREPARATION OF NEOPTERIN IMPRINTED NANOFILM COATED SURFACE PLASMON RESONANCE SENSORS FOR DETECTION OF NEOPTERIN FROM HUMAN SERUM

Burcu EREN YÜNGEVİŞ

Department of Bioengineering

Supervisor: Prof. Dr. Gözde BAYDEMİR PEŞİNT

July 2022, 54 pages

Neopterin (Neo) is produced by induction of macrophages by T-lymphocytes that activate interferon-gamma (IFN-ϒ) from guanosine triphosphate (GTP). Neo is synthesized only in activated macrophages of humans and primates, and from there it passes to plasma. Neo is present in serum and urine at pronounced constant rates. For this reason, it can be a useful marker for monitoring infectious disease activity during treatment and for estimating the extent of the disease and prognosis. Our aim in this study is to selectively detect Neo from body fluids by synthesizing Neo-imprinted nanofilms on the gold SPR chip surface. First, after cleaning the gold-coated chip surface with piranha solution, the surface will be modified by dropping allyl mercaptan. Then, using HEMA-EGDMA and AIBN, a molecularly imprinted polymer solution will be prepared and the SPR will be poured onto the chip surface to obtain a nanofilm surface under appropriate conditions. In addition, initial Neo concentration, interaction time and selectivity for chip surfaces will be investigated. SPR studies will be carried out using gold chips with a Neo imprinted (Neo-MIP SPR chips). For this, Neo-MIP SPR chips will be prepared and then the selective recognition of Neo will be tested using the SPR sensor.

Keywords: Nanofilm, Molecular Imprinted Nanofilms, Neopterin.

ÖZET

İNSAN SERUMUNDAN NEOPTERİN TESPİTİ İÇİN NEOPTERİN BASKILI NANOFİLM KAPLI YÜZEY PLAZMON REZONANS SENSÖRLERİNİN HAZIRLANMASI

Burcu EREN YÜNGEVİŞ
Biyomühendislik Anabilim Dalı
Danışman: Prof. Dr. Gözde BAYDEMİR PEŞİNT
Temmuz 2022, 54 sayfa

Neopterin, (Neo) guanozin trifosfat (GTP)'tan interferon-gamayı (IFN-ϒ.) aktive eden T-lenfositlerce makrofajların indüksiyonu ile üretilir. Neo, sadece insanların ve primatların aktive olmuş makro fajlarında sentezlenir ve buradan plazmaya geçer. Neo, serumda ve idrarda belirgin sabit oranlarda bulunur. Bu nedenle, tedavi sırasında bulaşıcı hastalık aktivitesinin izlenmesinde ve hastalığın yaygınlığının ve prognozunun tahmin edilmesinde faydalı bir belirteç olabilir. Bu çalışmada amacımız, altın SPR çip yüzeyi üzerinde Neo baskılanmış nanofilmler sentezleyerek vücut sıvılarından Neo'yu seçici olarak tespit etmektir. İlk olarak, altın kaplı çip yüzeyi piranha solüsyonu ile temizlendikten sonra allil merkaptan damlatılarak yüzey modifiye edilecektir. Daha sonra, HEMA-EGDMA ve AIBN kullanılarak moleküler baskılanmış polimer çözeltisi hazırlanacak ve SPR çip yüzeyine dökülerek uygun koşullarda nanofilm yüzeyi elde edilecektir. Ayrıca bu çip yüzeyleri için, başlangıç Neo konsantrasyonu, etkileşim süresi ve seçicilik araştırılacaktır. SPR çalışmaları, Neo baskılı nanofilm yüzeyine sahip altın çipler kullanılarak gerçekleştirilecektir. Bunun için Neo baskılanmış SPR çipleri hazırlanacak ve daha sonra Neo'nun seçici olarak tanınması, SPR çipi kullanılarak test edilecektir.

Anahtar Kelimeler: Nanofilm, Moleküler Baskılı Nanofilmler, Neopterin.

ACKNOWLEDGEMENTS

To my supervisor, Prof. Dr. Gözde BAYDEMİR PEŞİNT, who always supported me throughout my graduate education, enlightened my path with his vast knowledge and experience, and shared my good and bad moments

Thanks to Okan ZENGER, İpek CANATAR, Pırıl ARISOY, Ece KAYA and Kardelen CEMEK for helping me to work in a warm and friendly environment during my studies.

To my dear friend Cansu ÇAPRAZ, whom we have known for many years, who always supported me and whose presence I always felt by my side,

To my best friend and husband Çağrı YÜNGEVİŞ for his moral support during my studies,

To my mother Aslı EREN and my father Şaban EREN, who supported me throughout my life and always stood by me in good days and bad.

Thank you...

This thesis was financially supported by ATU BAP Coordination Unit with project number of 21303001.

TABLE OF CONTENTS

LIST OF FIGURES

LIST OF TABLES

NOMENCLATURE

ABBREVIATIONS

Neo : Neopterin

HEMA : 2-hydroxyethyl methacrylate

EGDMA : Ethylene glycol dimethacrylate

AIBN : Azobisisobutyronitrile

SPR : Surface Plasmon Resonance

FTIR : Fourier Transform Infrared Spectroscopy

AFM : Atomic Force Microscope

MIPs : Molecular Imprinted Polymers

BH_4 : Tetrahydrobiopterin

NH_2P_4 : 7,8-dihydroneopterin triphosphate

APC : Antigen-presenting cells

IFN- γ : İnterferon-γ

APS : Ammonium persulfate

RI : Refractive index

GTP : Guanosine triphosphate

HPLC : High performance liquid chromatography

ELISA : Enzyme Linked Immunosorbent Assay

RIA : Radioimmunoassay

LOD : Limit of detection

MAA : Methacrylic acid

TGA : Thermogravimetric analysis

TEM : Transmission Electron Microscopy

ADVN : 2,2'-azobis-2,4-dimethylvaleronitrile

DVB : Divinylbenzene

ICONS

ΔR : Delta reflection

R_{max} : Maximum SPR signal shift

C : Analyte concentration

ka : Binding rate constant

kd : Separation rate constant

K_A : Binding constant

K_D : Dissociation constant

1/n : Freundlich surface heterogeneity index

k : Selectivity coefficient

k' : Relative selectivity coefficient

1. INTRODUCTION

Neopterin (Neo) can be detected in body fluids such as serum, cerebrospinal fluid, synovial fluid, etc., so it is possible to diagnose immune diseases by examining elevated levels of Neo in the body (Hammerlink, 1999; Beldowska & Zwirska-Koeczala, 2001). Neo is a type of pteridine that is biosynthetically derived from guanosine triphosphate and has a molecular weight of 253 g/mol. It is considered a biomarker for a proinflammatory immune response. Elevated concentrations of Neo in body fluids such as serum or urine indicate activation of cellular immunity (Beldowska & Zwirska-Koeczala, 2001). One can observe this increase in viral and bacterial infections, malignancies, HIV, rheumatoid arthritis, Lyme disease, malaria and many other pathological diseases. (Centi et al., 2015; Sucher et al., 2010)

Molecularly imprinted polymers (MIPs) can be prepared for the detection of substances such as inorganic substances. Compared to natural biomolecules, their advantages such as specificity, stability and low cost come to the fore (Piletsky & Turner, 2006). Thanks to these properties, they have become an important alternative to natural bioreceptors used in sensing applications. The change in refractive index in surface plasmon resonance (SPR) sensors, the change in mass in acoustic sensors, and the change in electrochemical impedance in electrochemical sensors, as well as the binding of the target analyte to MIP, are analyzed (Piletsky et al., 1998).

By improving binding kinetics, analysis time is reduced, and by removing most of the template, MIPs are successfully used in sensing technology. In the development of nanoscale MIPs, the surface area to volume ratio is increased, making the binding sites more accessible to the analytes (Malitesta et al., 2012). MIP nanoparticles (Neos) and nanofilm surfaces have been incorporated into instrument design using various formulations and have been successfully used in a variety of analytical applications (Wackerlig &Lieberzeit., 2015).

SPR is an excellent method for measuring changes in refractive index near the metal surface. (Homola, 2008). SPR-based biosensors can be used to measure interactions between biomolecules without the need for labeling. Because they are able to measure interactions simultaneously and directly, they allow the determination of kinetic or thermodynamic parameters, concentrations, or ligand-analyte interactions. Because SPR-based biosensors have a fast response time and high selectivity, they can be used to understand a variety biomolecular

mechanisms, from protein-protein, antibody-antigen, receptor-ligand interactions to the identification of low molecular weight compounds (Homola, 2008).

In this study, a molecularly imprinted SPR-based biosensor was prepared for the determination of Neo. For this purpose, Neo molecules were firstly interacted with VIM and the resulting precomplex was prepared together with the polymerization solution and imprinted on the surface of the SPR sensor chip. At this stage, a non-imprinted SPR sensor chip was also prepared. Atomic force microscopy (AFM), contact angle and FTIR spectrophotometer were used to measure the surface characterization of the prepared SPR chips, and as a result of AFM measurements revealed that the Neo molecule was imprinted in a monolayer near the surface. Adsorption studies were performed with the prepared sensors and they were found to be very sensitive to Neo.

In addition, the interactions of the prepared sensors with Pterin and Glucose and their selectivity for Neo molecules were studied. Finally, Neo was determined from the natural source using plasma samples diluted to varying degrees, which is a natural source of Neo, and it was found that the sensor can measure even at high dilution rates in this complex environment where many proteins are present.

2. LITERATURE REVIEW

2.1. Pteridines

Pteridines were first isolated from a biological material in 1889. At that time studies on pteridines began and they were defined as pigments of insects and vertebrates. (Müler et al 1991). Interest in pteridines has increased following several findings. These include the recognition that tetrahydrobiopterin (BH4) is a cofactor of aromatic hydroxylase, the detection of conjugated disorders in BH4 metabolism that can lead to hyperphenylalaninemia, and the detection of changes in urinary pteridines (especially Neo) in individuals with malignancies and infectious diseases (Tomandl et al., 2003). In addition, pteridines serve as cofactors in many enzyme-catalyzed reactions, particularly in the transfer of single carbon fragments of tetrahydrofolate and tetrahydromethanopterin and in various redox reactions such as molybdopterin xanthine dehydrogenase (Baracher et al., 1998).

Pterins are a group of compounds known as pteridines. Pteridines have the pyrazino[2,3,d]pyridine structure. When the oxo group in the fourth position of amino is in the second position of the pteridine ring, the structure is called pterin (Wachter et al., 1989). Pteridines are divided into two groups: conjugated pteridines and unconjugated pteridines. Conjugated pteridines are known as folates bound to p-aminobenzoyl glutamates. They play important roles as cofactors in thiamine synthesis, amino acid metabolism, purine and pyrimidine synthesis, and single carbon atom transfer (Nichol et al., 1985). In the non-conjugated pteridines, the carbon in the sixth position of the pteridine molecule contains a simple hydroxyl alkyl group (Gieseg & Cato, 2003). The chemical structure of pteridines detected in human tissues and body fluids is listed in Table 1. Neo belongs to this group (Tomandl et al., 2003).

Table 1. Pterins detected in human tissues and body fluids

COMPOUND	**SIDE CHAIN**
Biopterin	C-6-CHOH-CHOH-CH3
7,8 - Dihidrobiopterin	C-6-CHOH-CHOH-CH3

Tetrahidrobiopterin	C-6-CHOH-CHOH-CH3
Neopterin	C-6-CHOH-CHOH-CH2OH
7,8 - Dihidroneopterin	C-6-CHOH-CHOH-CH2OH
Sepiapterin	C-6-CHOH-CHOH-CH3
İzosepiapterin	C-7-CHOH-CHOH-CH3
Ksantopterin	C-6-OH
İzoksantopterin	C-7-OH
6-Karboksipterin	C-6-COOH

2.2. Neopterin

Neopterin (Neo) was first found in the larvae of bees in 1963 (Turgan et al., 2001). In humans, the presence of Neo was first detected in urine by Sakurai and Goto in 1967 (Sakuari et al 1967, Hyland et al., 1988, Beigel, 2005). Wachter et al. discovered in their work that people with malignancies had high concentrations of Neo in their urine excretions (Wachter et al., 1989). They hypothesized that the high Neo concentration might be related to the activation of the immune response against tumors and viral cells in the human body (Piletsky & Turner, 2006). Huber and colleagues, on the other hand, discovered in their studies that activation of the cellular immune response causes an increase in Neo concentration in the human body (Hammerlink, 1999; Huber et al., 1984; Huber et al., 1983). The positive results of these studies led to intensive investigation of the use of Neo as a biomarker for disease (Sucher et al., 2010).

The main source of Neos in humans is monocytes/macrophages, but Neo is also secreted by microglial cells and the central nervous system. Neo is synthesized from guanosine triphosphate (GTP) by the catalytic action of the enzyme guanosine triphosphate (GTP) cyclohydrolase I through interferon-γ (IFN- γ) released by T lymphocytes in active macrophages/monocytes. It is known that the activity of the enzyme GTP-cyclohydrolase-1 increases with the increase of

IFN-γ action. In the next step, 7,8-dihydroneopterin triphosphate is converted to 5,6,7,8-tetrahydrobiopterin (BH_4) by catalysis of the magnesium-dependent 6-pyruvoyl-tetrahydropterin synthase (PTPS). This step does not occur in monocytes, macrophages, and endothelial cells, which lack 6-pyruvoyl-tetrahydrobiopterin synthase. Neo is formed by oxidation of the elevated 7,8-dihydroneopterin triphosphate (Hoffmann et al., 2003).

Neo is a clinically used marker of cellular immunity in a variety of disease groups. Alterations in neo levels were first noted in malignancies and viral infections (Castro et al., 2004). Neo is a pteridine derivative released by human monocytes and macrophages via interferon gamma, whose biological function is not fully understood and which has no specific receptor (Zimmerman et al., 2005; Widner et al., 2002). Interferon gamma released by active helper T lymphocyte cells induces macrophages to produce and release Neo into body fluids (Zwetkova et al., 2001). Thus, oxidative stress caused by immune system activation is assessed by the Neo level. It is known that the level of Neo increases 3 days before T-cell proliferation and 1 week before antibody production. Because of these properties, Neo can be used to assess cellular immune response as well as to diagnose and monitor diseases related to the immune system (Durukan et al., 2004).

Neo has been detected in serum, cerebrospinal fluid, synovial fluid, urine, semen, pancreatic fluid, and saliva (Widner et al., 2002; Durukan et al., 2004; Wirleitner et al., 2003; Ormazabal et al., 2005). Since Neo cannot enter the vein and is excreted unchanged by the kidneys, urinary Neo levels and interferon-gamma levels are evaluated indirectly (Durukan et al., 2004). Neo levels increase during pregnancy, especially in the last weeks of pregnancy. Neo concentrations in newborns are three times higher than maternal levels. This is because there is an increase in monocyte/macrophage activation during pregnancy (Hammerer-Lercher et al., 2006). Measurement of Neo can be performed by methods such as HPLC (high performance liquid chromatography), ELISA (enzyme linked immunosorbent assay), and RIA (radioimmunoassay) (Westermann et al., 2000). It is believed that there is no Neo loss when separating plasma or serum from venous blood samples. Serum and plasma Neo levels are stable for up to three days at room temperature and in a dark place. If the serum is to be stored longer, it can remain stable at -20 °C for up to three months and at -80 °C for up to one year.
The level of Neo in the serum of healthy adults ranges from 2.6-8.7 nmol/L and the upper limit of this level is assumed to be 10 nmol/L. Although serum Neo concentrations are higher in the

elderly and children, they have been reported not to depend on sex (Buehrer-Sekula et al., 2000).

2.2.1. The Chemical Structure of Neopterin

Neo, which has the closed formula $C_9H_{11}N_5O_4$, has a low molecular weight (253.32 g/mol) and is a pteridine compound known by the chemical formula 2-amino-6-(1,2,3-trihydroxypropyl)-4(3H)-pteridinone (Widner et al., 2002). Its chemical structure is shown in Figure 1. It has four isomers, D-erythro, L-erythro, D-threo, and L-threo. The derivatives of D-isomer are important for human metabolism and are found in the body as dihydroneopterin and tetrahydroneopterin. It shows strong fluorescence in neutral or alkaline environments and weak fluorescence in acidic environments (Budavari et al., 1976; Fuchs et al., 1992). The D-isomer of Neo is found only in humans and primates and plays an important role in metabolism (Abate et al., 1989).

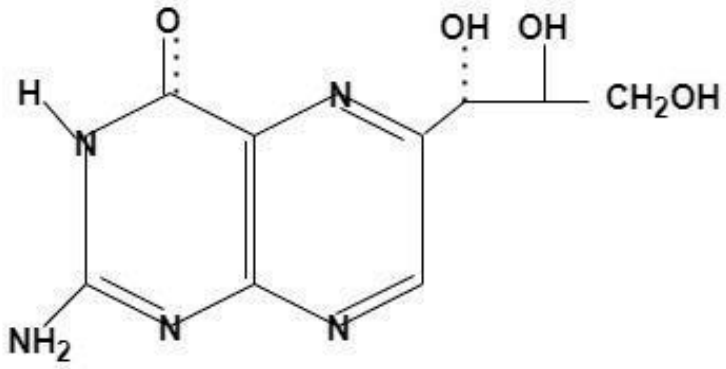

Figure 1. Chemical representation of Neo

2.2.2. Biosynthesis of Neopterin

Neo is produced by monocytes and macrophages activated from GTP by the enzyme GTP cyclohydrolase I (GCH-I). GCH-I is an enzyme that plays a key role in the biosynthesis of pteridine. The activity of GCH-I enzyme is largely regulated by IFN-gamma and to a lesser extent by other cytokines and IFN-gamma. IFN-gamma is released by active T helper type 1 (Th-1) lymphocytes (Widner et al., 2002; Razumovitch et al., 2003). These cells are the strongest triggers of Neo production. GTP first converts to an intermediate, 7,8-dihydroNeo triphosphate (NH_2TP) (Widner et al., 2002). Neo is a pyrazine-pyrimidine compound, 2-amino-4-hydroxypterine of low molecular weight. NH_2TP is converted to 7,8-dihydroneopterin and Neo by the enzyme phosphatase. NH_2TP is also converted to 5,6,7,8-tetrahydrobiopterin (BH_4) by the enzymes 6-pyruvoyl-tetrahydropterin synthase (PTPS) and sepiapterin reductase. In the

presence of the enzyme dihydropteridine reductase, BH_4 forms the final product Biopterin (Werner et al., 1991).

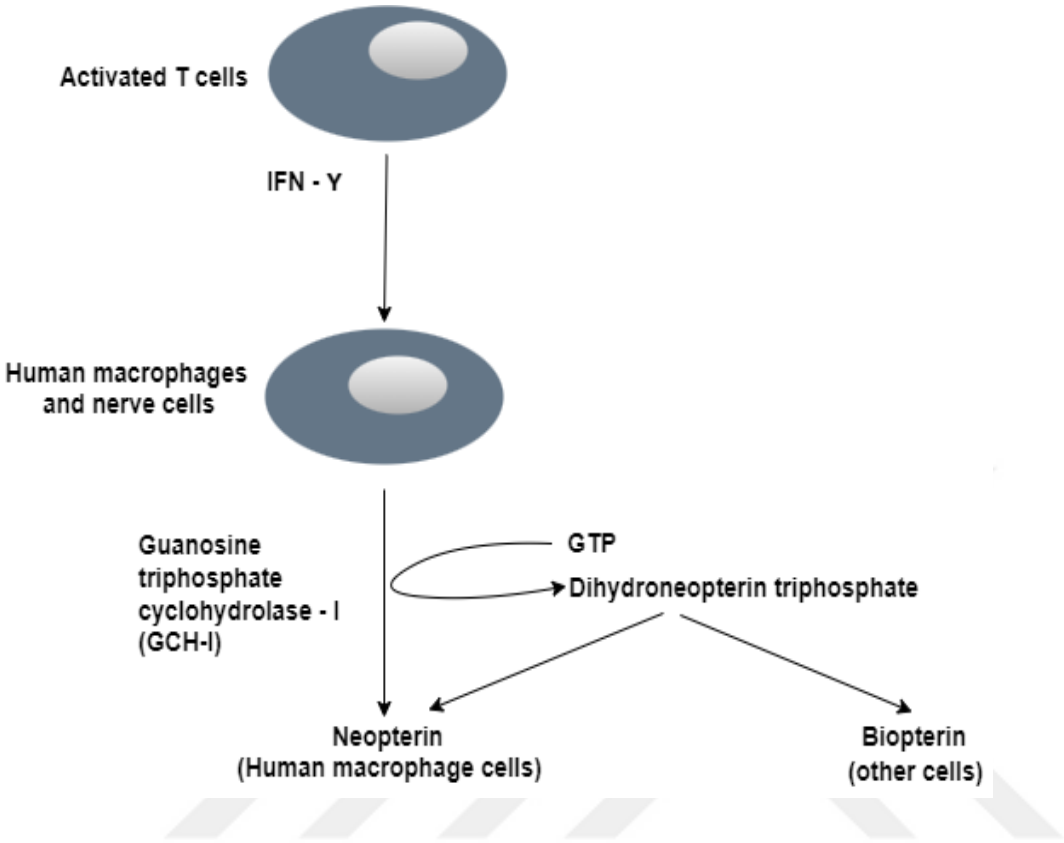

Figure 2. Neo synthesis steps in humans

2.2.3. The Immunological Role of Neopterin

All reactions of a living being that is able to recognize molecules against pathogens constitute the immune system. Foreign pathogens that invade the host organism are recognized by antigen-presenting cells (APC) and presented to T/B lymphocytes. APC cells confronted with thymus-dependent antigens release IL -1 while presenting the antigen to Th lymphocytes (T helper lymphocytes), causing these lymphocytes to proliferate and secrete lymphokines. Thymus-independent antigens are presented directly to B lymphocytes. Th lymphokines stimulated by APC differentiate T-/B-lymphocytes and allow the release of immune response products (Erganiş & İstanbulluoğlu, 1993; Müftüoğlu et al., 1993).

Measurement of Neo level allows determination of cellular immune activation resistance. The cellular immune system plays a central role in the initiation and development of many common diseases, especially viral infections, autoimmune diseases, other inflammatory diseases, transplant rejection, and cancer (Çaksen et al., 1998). Concentrations of Neo have been

determined in various diseases and have been found to correlate with concentrations of other cytokine immune activation markers such as sTNF-R, sIL-2R, and INF -γ (Widner et al., 2000). The presence of elevated Neo concentrations in body fluids of malignant and viral patients has led to the study of Pteridin synthesis associated with the immune system. (Werner et al., 1991). Elevated Neo concentrations in serum and urine of patients with malignant and viral infections can be used as diagnostic and prognostic criteria for cell-mediated immunity (Akgul et al., 2013).

The level of Neo responds rapidly to immunological stimulation. INF -γ is released by active T helper lymphocytes type 1 and natural killer cells. The released INF-γ activates macrophages and stimulates the GCH-1 enzyme in the GTP-biopterin pathway, resulting in high production of Neo (Horak et al., 1998; Widner et al., 1998). Therefore, INF -γ is one of the strongest triggers for the production of Neo. Elevated Neo concentrations in body fluids indicate increased INF -γ stimulation. (Vrecko et al., 1997; Müller et al., 1998).

2.2.4. Neo in Body Fluids

Neo is a low molecular weight substance that is biologically and chemically stable in body fluids and can be detected by routine measurements in the laboratory environment during immune response. Neo is excreted by the kidney, and changes in Neo concentration in serum are reflected in urine as long as renal function is not impaired (Fuchs et al., 1994). In addition, Neo can be determined from various body fluids such as serum, cerebrospinal fluid, synovial fluid, urine, pancreatic fluid, and plasma (Berdowska et al., 2001).

The serum level of Neo is accepted as an upper limit of 10 nmol / L in healthy adults. Due to its low molecular weight, Neo is excreted by the kidneys without changing its original structure. It has been reported that changes in concentrations in serum Neo cause a parallel change in concentrations in urine Neo (Ozmeric et al., 2002). A positive correlation has been observed between concentrations of Neo in urine and Neo in serum (Putzki et al., 1987; Denz et al., 1990). Since Neo is also somewhat sensitive to direct sunlight, samples must be protected from light during transport and storage. Generally, wrapping the samples in aluminum foil is sufficient. Alternatively, you can use dark colored tubes to collect the samples. In addition, a decrease in the amount of Neo can be observed during thawing and freezing. Serum and plasma levels of Neo are stable for up to three days at room temperature and in a dark place. If stored

longer, they are stable for up to three months at -20°C and up to one year at -80°C (Fuchs et al., 1992).

Levels of Neo in urine are determined from creatinine levels (Bichler et al., 1983). Normal levels of Neo in urine are 50-250μmol Neo / mol creatinine (Müler et al., 1991). It has been observed that the average Neo / creatinine ratio is lower in men than in women. It has been reported that this difference is due to the higher creatinine levels in males compared to females (Watcher et al., 1989).

CSF Neo concentrations do not differ by sex. CSF Neo is 4.2 ± 1.0 nmol / L in healthy adults (Plata-Nazar & Jankowska, 2011) Improper collection, storage, and processing of CSF samples will result in lower readings than the current Neo concentrations. This problem is solved by collecting CSF samples in tubes containing 1 mg / ml dithioerythritol (DTE) and 1 mg / ml acetylenetriaminepentaacetic acid. CSF collected in this manner remains stable at room temperature for more than one year and two hours after thawing.

2.3. Detection Methods of Neopterin

The content of Neo in body fluids can be determined by ELISA, RIA, electrophoresis, GC-MS, column and paper chromatography, thin-layer chromatography, HPLC fluorescence, or electrochemical detectors. In this study, the rapid and simple detection of Neo was aimed using surface plasmon resonance. (Hyland et al., 1988; William et al., 1998; Biacore, 2003). According to best of our knowledge, Neopterin detection via SPR sensors studied for the first time, in this thesis.

2.3.1. HPLC

HPLC was discovered in the mid-1970s and rapidly evolved with the development and use of column filling materials and online detectors. Chromatographic analysis of pterins in today's clinical laboratories is based almost exclusively on HPLC techniques, and most studies require measurement of Neo and biopterin in various diseases. Fluorescence or electrochemical detection is used to separate these pterins by cation exchange, reversed-phase, or reversed-phase ion-pair chromatography (Fuchs et al 1992).

2.3.2. Fluorescence Detection

The fluorescence detection method has the necessary sensitivity and selectivity to measure pterins in biological samples. Most, if not all, oxidized pterins fluoresce, and it is a problem that they are endogenous in their reduced form. In this respect, the reduced pterins must be chemically converted to the oxidized form before analysis (Fuchs et al 1992, Zhang et al 2020). Using a method in which pterins are oxidized differently by iodine under acidic and alkaline conditions, the three oxidation states of biopterin, dihydrobiopterin, and tetrahydrobiopterin can be measured (Fuchs et al 1992).

2.3.3. Electrochemical Detection

Since fluorescence detection does not allow direct measurement of reduced pterins, various oxidation processes are used to estimate the concentrations of reduced pterins. The electrochemical detection method is a direct analytical method of oxidized and reduced endogenous pterins in biological samples (Fuchs et al 1992, Zhang et al 2020)

2.4. Surface Plasmon Resonance (SPR)

SPR technology has been used since 1982, almost four decades ago. Since its first observation by Wood in 1902, the physical phenomenon of surface plasmon resonance has found its place in sensitive detectors and in practical applications (Wood, 2009, Wood, 2010). When Wood reflected polarized light through a mirror, he observed anomalous band patterns in the reflected light in the dark. The physical interpretation of this phenomenon was initiated by Lord Rayleigh (Rayleigh, 1907) and later elucidated by Fano (Fano, 1941).

However, complete clarification was not possible until Otto (Otto, 1968) published studies on the stimulation of surface plasmons in 1968 and Kretschmann and Raether (Kretschmann and Raether, 1968) in the same year. Applications for the study of biomolecular interactions of SPR-based sensors were first initiated by Liedberg et al in 1983 (Liedberg et al.,1983). SPR biosensors have developed rapidly since their first use as an effective alternative for the analysis of biological interactions. There are many research articles reporting SPR biosensors and their applications in protein immobilization. (Bai et al., 2012; Park et al., 2011; Oliveira et al., 2011).

2.4.1. Physical Basis of SPR

SPR is a highly sensitive and label-free optical analysis method and consists of parts such as an optical unit, a liquid unit and a sensor chip integrated into the system (Puiu and Bala, 2016;

McWhirter et al., 2008; Biacore, 2003). The sensor chip acts as a physical barrier between the liquid cell and the optical unit, and biomolecular interactions take place in the liquid part of the SPR sensor Victoria (2012).

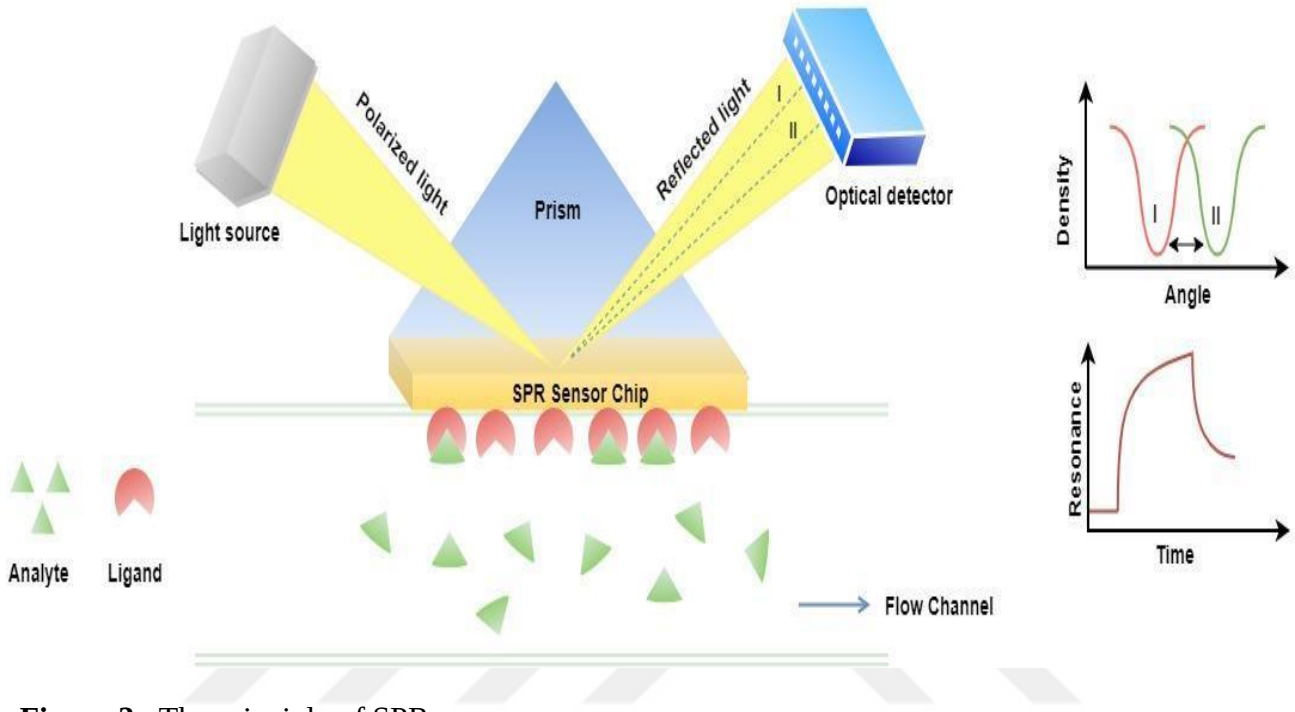

Figure 3. The principle of SPR

The SPR technique, gold etc. exploits the properties of the materials. The thin layer of gold applied to a material with a high refractive index absorbs the laser beam, and electron waves are generated on the gold surface. The receiver (receptor) is sent to the structure to be analyzed using fluid channels. When the receptor is connected, the behavior of the light on the surface of the gold layer changes, resulting in a change in the refractive index. Thanks to this optical change, qualitative and quantitative measurements can be performed with high precision and in real time, without the need to label biological interactions (Chang et al., 2018; Altintas, 2018)

The surface of the SPR sensor is sensitive to environments as small as 300 nm. The design of the microflow cell should be well controlled, reproducibility studies should be performed, and a small sample volume should be used (Puiu and Bala, 2016). The SPR angle is based solely on the refractive index (or dielectric constant) of the medium. (Maier, 2007; Dastmalchi et al., 2016). The refractive index (RI) of the dielectric medium changes depending on parameters such as ligand-receptor binding, temperature changes, and chemical reactions. (Erickson et al., 2007; Nguyen et al., 2015; Kihm et al., 2012).

Temperature changes have a great impact not only on the response of SPR, but also on the affinity of biomolecular interactions and kinetics. Moreover, according to the working principle of SPR, the interaction of light with metal is taken into account, and the resolution and sensitivity of SPR-based sensors depend on the properties of the metallic surface (thickness, structure, etc.) Scarano et al (2010).

2.4.2. SPR Biosensors

Figure 4. SPR-based biosensor

SPR-based biosensors provide information on non-covalent interactions of biomolecules such as protein-protein interactions, enzyme-substrate, antibody-antigen, protein-nucleic acids, and protein-polysaccharides (Erickson et al., 2007; Altintas, 2018). SPR analyzes detect protein-protein, protein-virus, enzyme-substrate or antibody-antigen, protein-DNA, drug, and protein-polysaccharide binding in real time Puiu and Bala (2016) and determine the association and dissociation rates during binding (Victoria, 2012; Homola, 2006). In addition, SPR-based biosensors can directly and easily measure biospecific interactions in real time without the need for chemical labeling (Jena et al., 2019).

In addition to the above advantages, the SPR biosensor is easy to use and set up by Chang et al. (2018). SPR technology offers high detection sensitivity, especially for direct detection of low concentrations of small molecules Chavanieu and Pugnière (2016). Although traditional methods such as PCR, culturing, and enzyme immunoassays are used for macromolecule

detection, these assays are time-consuming. Recently, SPR technology has been preferred in place of these methods. (Prawobo, 2017; Farka et al., 2016).

SPR-based detection technology offers a bright future in biosensor diagnostics if the nonspecific binding problems in human samples and the limited penetration of the sensor are overcome Altintas (2018). The detection limit (LOD) of biomaterial applied to the sensor surface is estimated to be 1 pg-mm-2 with SPR Biacore (2003). This sensitivity is sufficient for biomolecules containing antibodies, proteins, or high molecular weight compounds such as DNA Justino et al. (2010). However, sensitivity studies are required for low molecular weight targets (less than 500 Da), bacteria, and very low levels of pathogenic viruses. The sensitivity and LOD of SPR sensors can be enhanced with nanostructured substrates and modified gold nanoparticles Helmerhorst et al. (2012).

2.4.3 Application Areas of SPR Biosensors

SPR technology is used in conjunction with biomarkers in the diagnosis of serious diseases such as heart disease, infectious diseases, and cancer. Most SPR biosensors for disease detection and diagnosis have standards tailored for use in a clinical setting and are in the prototype stage Altintas (2018). However, by producing these devices at pilot scale, effective and rapid diagnostics can be developed to help control epidemic diseases. Rapid diagnosis confirms clinical suspicion of infection and guides further treatment and prognosis. This will reduce healthcare costs and enable early public health intervention to prevent the spread of pathogens Shi et al. (2015). The benefits of SPR sensor technology are clear: physicians can quickly identify a specific pathogen and recommend an appropriate treatment method Caygill et al. (2010).

Laboratory methods such as microscopy, nucleic acid amplification, and immunological tests are commonly used to detect disease. Usually, these methods take a lot of time and have unintended consequences. Another drawback is the need for highly skilled personnel to perform these methods Altintas et al. (2011). New technologies such as SPR-based biosensors are being developed for faster and easier detection and diagnosis of diseases Altintas (2018).

In a 2010 study, Zybin and colleagues investigated the binding of a single nanoparticle to the sensor surface using the SPRi technique to demonstrate the binding of SPR-based nanoparticles (80 nm in diameter) to the functional gold sensor surface. In addition, in this study, the binding

of HIV virus-like particles (with a diameter of about 100 nm) to the antibody-coated sensor surface was also observed Zybin et al. (2010). The proposed experimental setup allowed monitoring of binding events over a relatively large surface area of the sensor (up to 10 mm2) and thus the sensitivity of the SPRi technique at high concentrations (Victoria, 2012; Zybin et al., 2010).

A study developed a simple platform for rapid and sensitive detection of H7N9 virus using an integrated IM-SPR biosensor with a newly produced monoclonal antibody. It was shown that the virus H7N9-RG, which has similar surface properties to avian influenza virus A H7N9, can be detected in as little as 10 minutes. Moreover, the detection limit is 402 copies/ml in mimic solution and much better results were obtained than with methods such as ELISA, commercial RIDT or even qRT-PCR Chang et al. (2018). A significant decrease in mortality has been observed with early diagnosis of patients infected with avian influenza A H7N9 virus, and the biosensor IM-SPR has been shown to have the potential to be an effective diagnostic platform (Zhang et al., 2013; Ge et al., 2013).

In another study, a DSU/amine-functional SPR-based rGO-PAMAM thin-film sensor was developed for the detection and quantification of DENV 2 E proteins. The results show that the developed sensor can successfully monitor changes in SPR angle while detecting the lowest concentration of DENV2 E proteins, 0.08 pM, within 8 minutes. The sensitivity and binding affinity constants of the developed sensor were measured to be 0.2576/pM and 7.6452 TM -1, respectively. The selectivity of the proposed sensor was also demonstrated, as the developed sensor was sensitive to DENV2 E proteins compared to DENV1 E proteins and ZIKV (Zika virus) E proteins. Overall, the rGO-PAMAM thin film-based SPR sensor with Au/DSU/Amin functionality was found to have the potential to serve as a rapid clinical diagnostic tool for DENV infections Omar et al. (2020).

2.5. Molecular Imprinting

Researchers have conducted selective and sensitive analytical experiments to develop faster and more efficient methods for use in medicine and biotechnology. Among the separation systems based on molecular recognition, carriers prepared by the "molecular imprinting" method are very promising due to their high selectivity for the target molecule. The "molecular imprinting" method, first defined by Günter Wulff and his research group in 1972, was used to

obtain highly selective binding sites by arranging the three-dimensional structures of functional groups in synthetic polymers (Wulff et al., 1987).

Bioreceptors such as antibodies are popular ligands used to purify specific antigens because of their high selectivity. However, these biological molecules with high selectivity are easily affected by environmental conditions and protein structures are denatured under acidic conditions, high temperatures, or as a result of proteolytic activity. The technique that transfers the recognition mechanism of biological systems such as antibody/antigen or enzyme/substrate to polymeric structures is called "molecular imprinting" (Mosbach, 1996).

The method of molecular imprinting consists essentially of three steps. In the first step, suitable monomers containing functional groups and capable of polymerization form a complex by binding to the template or, in other words, to the target molecule through covalent or non-covalent interactions so that pre-structuring can take place. In this step, a structure is formed around the mold in which the functional monomer is bound. The three-dimensional structure and chemical properties of the target molecule play an important role in this interaction. In the second step, the monomer-template complex is polymerized over the functional monomer using a suitable crosslinking agent. In the third step, the molding molecule is removed from the polymer to create interstitial spaces in the structure that will replace the target molecule. Under favorable conditions, these interstices recognize the size, structure and physicochemical properties of the template molecule and bind the template molecule selectively and effectively. The selectivity of the polymeric adsorbent in ion imprinted processes that use ions as templates. It is based on the charge, size, coordination number and geometry of the suppressed ion (Cormack & Mosbach, 1999). The ion suppression method has been used in many studies of metal ion adsorption (Yavuz et al., 2005; Andaç et al., 2004; Ersöz et al., 2004; Say et al., 2003a; 2003b).

Molecularly imprinted polymers (MIPs) have become a favorite of researchers because they represent a new type of adsorbent and possess attractive properties such as ease of preparation, stability, low cost, and molecular recognition. The molecular imprinting method is basically divided into two types: covalent imprinting and non-covalent imprinting, depending on the type of bond formed between the functional monomer and the template molecule (Mujahid & Dickert, 2016).

2.5.1. Covalent Imprinting

Before the polymerization process, the functional monomer and the template molecule are linked by covalent bonds. After the polymerization process, the covalent bonds are broken and removed from the polymer to form a mold. The same covalent bond is formed again when the target molecule interacts with the imprinted polymers (Shea & Doughertly, 1986).

Although the monomer-molecule complex has advantages, such as being quite stable and occurring in stoichiometric ratios, polymerization conditions (such as high temperature, high or low pH, and polar solvents) can be applied as desired, there can often be problems in synthesizing the monomer-molecule conjugate, and the synthesis process is costly. In addition, the number of reversible bonds of the target molecule to the polymer is limited and the binding kinetics is slow due to the formation of covalent bonds (Yan & Kyung, 2006).

2.5.2. Non-covalent Imprinting

Bonding of the functional monomer and the template molecule occurs through non-covalent interactions (such as hydrogen bonding, electrostatic interactions, and the formation of coordination bonds). After polymerization, the mold molecule is removed from the polymer using suitable solvents. Polymers imprinted with the target molecule are bound by non-covalent interactions (Ersöz et al., 2004). The non-covalent imprinting technology has the advantage that the synthesis of the covalent monomer-mold conjugate is not required and that the mold molecule can be easily removed from the polymer after polymerization. This is because non-covalent interactions are weaker and the binding kinetics of the target molecule are fast. However, polymerization conditions are limited to increase non-covalent interactions. Functional monomers can be overused to increase the bond formation equilibrium, which can lead to the formation of non-specific binding sites (Zhang et al., 2006).

Both methods have several advantages over the other. The choice of method depends on the nature of the target molecule, its structure, the degree of selectivity, time, and cost. In the years when the technique of molecular imprinting was first used, imprinted polymers were synthesized by covalent interactions. Later, non-covalent interactions were investigated because they were easier to implement. Any type of polymerization technique (radical, anion, cation, and condensation) can be used for molecular imprinting. As long as the polymerization conditions do not damage the components (molds, crosslinking agents, non-covalent

interactions with the monomer and others). However, most radical polymerization techniques are used because of their ease of preparation and application (Wulff & Knorr, 2001).

The molecular imprinting process uses (1) functional monomers, (2) crosslinkers, (3) solvents for polymerization, and (4) initiators.

Functional monomers: In covalent imprinting, the template molecule is covalently bonded to vinyl groups. Acrylic acid amides and esters or methacrylic acid are the most commonly used monomers. In non-covalent printing, vinyl monomers linked to suitable functional groups are used (Yan & Kyung, 2006).

Crosslinkers: Divinylbenzene (DVB) and ethylene glycol dimethacrylate (EGDMA) are the most commonly used crosslinkers. The main function of these agents in printing is to create a stable structure around the mold molecule, in other words, they form a knitted structure. In addition, they prevent the printed polymers from dissolving in solvents. The use of different crosslinkers ensures that the structure of the binding sites of the template molecule is protected as well as the chemical environment. For an effective suppression process, the crosslinkers and the functional monomers must be compatible. Otherwise, one of the functional monomers or the cross linker will dominate during polymerization and copolymerization will not occur. The ratio of crosslinker to functional monomer is also important. If the molar ratios are too small, the binding sites of the template molecules will be too close to each other, the binding sites of the target molecule will be occluded by the neighboring regions, and an effective result cannot be obtained. At very high molar ratios, the effectiveness of the suppression is again reduced because the crosslinkers exhibit non-covalent interactions with functional monomers or the template molecule (Wloch & Datta, 2019).

Solvents: Solvents not only dissolve the polymerization agents, but also ensure that the imprinted polymers have a porous structure and increase the binding rate of the target molecule. The porosity of the structure also ensures that the bound target molecule is released from the polymer. During polymerization, the reaction temperature increases locally, causing the formation of undesirable by products. Another task of the solvents is to evenly distribute the heat of reaction during polymerization.

Initiators: Radical polymerization can be initiated by thermal degradation of radical initiators. Usually, 2,2'-azobis isobutyronitrile (AIBN) and 2,2'-azobis 2,4-dimethylvaleronitrile (ADVN) are used. In cases where the non-covalent interactions between the monomer and the template molecule are very weak, very high temperatures cannot be reached. Under these conditions, UV degradation is preferred to thermal degradation (Mjangos et al., 2006).

The highly selective recognition of substrates and their binding by the imprinted polymers depends on the physical and chemical properties of the material (such as flexibility, number of binding sites and structure of the material). For molecularly imprinted polymers to be more useful, not only the selectivity of the substrate must be important, but also the desorption and rebinding kinetics must be fast under suitable conditions. Therefore, the selection of appropriate binding interactions is very important in the development of molecularly imprinted materials. More than one binding site ensures that the interactions between the binding sites of the monomer and the template molecule are better, and thus the molecular recognition is more selective (Komiyama et al., 2003; Haupt, 2003).

The difference in molecular interactions affects the degree of selectivity and reversibility. For example, interactions generated by covalent bonds are highly specific, but the feedback kinetics are slow. In contrast, the kinetics of hydrophobic interactions are faster, but the selectivity decreases. In general, non-covalent interactions have a wider range of applications because of their applicability to many compounds, their fast kinetics, and their ability to form and break bonds under more favorable conditions. In addition, certain non-covalent interactions such as Π-Π interactions, hydrogen bonding, and metal coordination interactions hold promise for the design of new molecularly imprinted functional polymers in the future (Yan & Ramström, 2005; Mahony et al., 2005; Hall et al., 2005; Wei et al., 2006).

2.6. Neopterin Detection Studies

Sharma et al. reported the development of a potentiometric sensor for the detection of Neo using an MIP. 2,2'-Bitiophen-5-boric acid 2(cytosin-1-yl)ethyl p-bis(2,2'-bithien-5-yl)methylbenzene and 2,4,5,2',4',5'-hexa(thiophen-2-yl)- 3,3'-bitiophene were used to prepare the MIP film. For comparison, Neo non-imprinted (NIP) film was synthesised by the same procedure and the morphology of both electrodes was characterized by AFM. As a result of the analysis, Neo was

determined in the concentration range of 0.15-2.5 mM (38-633 ug/mL) with a detection limit of 22 µM (5.6 ug/mL). The sensor prepared in this study showed selectivity toward glucose and creatinine as well as toward 6-biopterin and pterin, which are structural analogues of Neo. In addition, Neo was determined from serum samples Sharma et al. (2016).

Neo is a useful biomarker for malignancy detection. However, work on adsorption using molecularly imprinted graphene oxide polymer material (GO-MIP) is lacking. In a study by Khoo et al, GO-MIP was synthesized and characterized for use in Neo adsorption study. Using methacrylic acid (MAA) as monomer, ethylene glycol dimethacrylate (EGDMA) as crosslinker, and ammonium persulfate (APS) as initiator, Neo was pressed by a free radical polymerization method. The binding sites of Neo were confirmed by analyzes such as Fourier transform infrared spectroscopy (FTIR), CHNS analysis, thermogravimetric analysis (TGA), field emission scanning electron microscopy (FESEM) and transmission electron microscopy (TEM). GO-MIP adsorbed twice as much Neo compared to the NIP and showed better selectivity towards the 6-biopterin molecule. The adsorption and its kinetic mechanism are described by the Freundlich isotherm and Lagergren's pseudo-square equation. The equilibrium adsorption capacity was determined to be 0.4749 mg/g at 10 mg GO-MIP, 1 mL Neo, 10 ppm conditions Khoo et al. (2019).

Huang et al. use Neo as a target molecule and then print it on poly(ethylene-co-vinyl alcohol) by solvent evaporation. After removing the template, the membrane is used as a sensing element for electrochemical urinalysis. It is a good alternative for developing a Neo detection system because it is inexpensive and highly sensitive, but selectivity studies have not yet been performed for this material. In addition, no reusability studies have been performed for the developed sensor chip. It has not been reported whether Neo can be detected with high selectivity over competing molecules that are structural homologs with Neo Huang et al., (2011).

There are studies in the literature for the detection of some molecules using molecular imprinting technique and SPR. For example, Akgönüllü et al. (2020) developed a surface plasmon resonance nanosensor, which is a highly sensitive and selective plasmonic detection method for the detection of AFB1. For this, AFB1 and N-methacryloyl-L-phenylalanine as template molecule and functional monomer were complexed and then molecular imprinted polymers with gold nanoparticles were coated on the SPR gold chip surface. As a result, the

AFB1 imprinted nanosensor showed a wide linear range between 0.0001 ng mL-1 and 10.0 ng mL-1, and the detection limit was calculated as 1.04 pg mL-1. When compared with the non-molecular imprinted nanosensor, the imprinting factor was determined to be 5.91. AFB1 detection studies were performed from various food samples. Finally, selectivity, reusability and storage stability studies were carried out for SPR nanosensors.

In another study, Yola et al. (2014) prepared a surface plasmon resonance (SPR) sensor for the detection of an important antibiotic, Amikacin (AMIK), in human plasma. After modification of the gold surface of the SPR chip with allyl mercaptan, AMIK imprinted poly(2-hydroxyethyl methacrylate-methacryloylamidoaspartic acid) [p (HEMA–MAAsp)] film was formed on the surface. Imprinted and unimprinted SPR chips were characterized by FTIR spectroscopy, AFM and contact angle measurements. As a result of the calculations, the linearity range of 0.01-0.15 g/mL and the detection limit of 0.0025 g/mL have been reached. Next, the developed AMIK imprinted nanosensor was successfully applied to human plasma samples for AMIK detection.

In another study, Bereli et al. (2021) developed a simple, fast and sensitive SPR sensor system for the determination of tartrazine (TA) from fruit juice products. Tartrazine imprinted and non-imprinted poly(hydroxyethylmethacrylate-N-methacryloyl-(L)-histidine methyl ester) thin films were synthesized on the SPR chip surface using ultraviolet polymerization. Kinetic studies were performed in the linear range of 0.5–100.0 μM and the detection amount for TA was found to be 0.0076 μM and the limit of quantitation 0.0252 μM. Selectivity studies of TA imprinted and non-imprinted SPR sensors were performed with allura red and sunset yellow molecules, with 7.21 and 5.76 times better selectivity results, respectively. The reusability of TA imprinted SPR sensors was found to be 85.20%. TA was successfully detected from juice samples using the SPR chip.

Detection studies of some molecules using the molecular imprinting technique and SPR are available in the literature, but there is no study in which these two methods are used together for Neopterin. This thesis is the first in this regard.

3. MATERIALS AND METHOD

3.1. Chemical materials

Ethylene glycol dimethacrylate (EGDMA), 2,2'-azobisisobutyronitrile (AIBN), 2-

Hydroxyethyl methacrylate (HEMA), vinylimidazole (VIM) used in polymerization and Neopterin (Neo), Pterin and Glucose used in selectivity studies were purchased from Sigma, USA. The reagents were stored at 4°C until use. All water used in the experiments was purified using a Millipore Direct-Q3V Ultrapure water purification system (MerckAG, Darm-stadt, Germany). Other chemicals used in the study were purchased from Merck, Germany in analytical purity.

3.2. Preparation of Neo-MIP and NIP SPR Nanosensors

3.2.1. Surface Modification of SPR Gold Chip

The SPR chip was cleaned by immersing it in 10 ml of acidic piranha solution (a mixture of ammonia (NH_4OH), hydrogen peroxide (H_2O_2) and water in a ratio of 1:1:3 (v:v:v) and waiting for 10 minutes. The SPR chip removed from the solution were washed with distilled water and ethyl alcohol and dried in a vacuum oven (200 mmHg, 45°C) for 1 hr. For the modification, 20 µL of allyl mercaptan was dropped onto the SPR chip and covered and left in the fume hood overnight. In the final step, the SPR chips were washed with ethanol and dried under nitrogen. As a result of the modification, SPR chip surfaces with bound allyl groups were obtained (Figure 5).

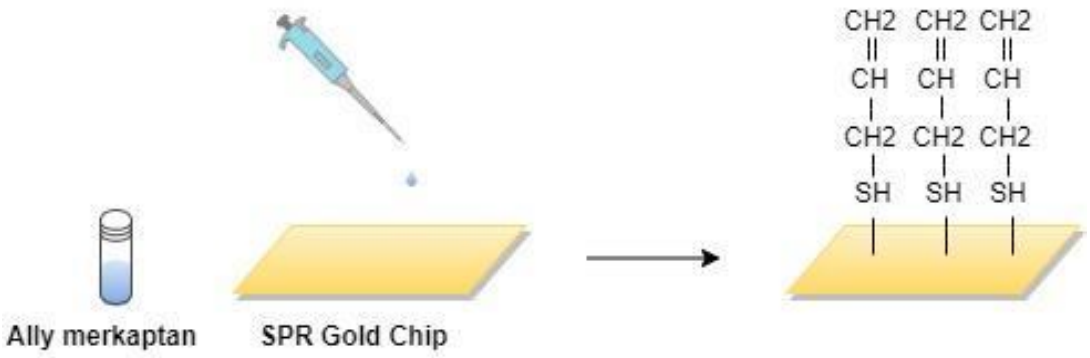

Figure 5. Surface Modification of SPR Chip

3.2.2. Preparation of Neo-VIM Precomplex

The Neo-VIM precomplex was prepared in water using Neo as the template molecule and VIM as the functional monomer. Six different amounts of monomer were studied (molar ratio of 1:3, 1:4, 1:5, 1:6, 1:7) and maximum Neo adsorption was achieved when the ratio of Neo-VIM was

1:5. A stoichiometric molar ratio of 1:5 was used in the preparation of the Neo-VIM precomplex, firstly 2.5 mg of Neo was weighed and 5 µl of VIM was added and dissolved in an ultrasonic water bath. It was then kept in the refrigerator for 4 hours to allow complexation to occur.

3.2.3. Preparation of Neo-MIP and NIP SPR Nanofilms

Neo-MIP SPR chips were prepared by polymerizing the Neo-VIM precomplex with the functional monomer HEMA and the crosslinker EGDMA. (400 µL) HEMA and (200 µL) EGDMA were added to the prepared precomplex. Dissolved O_2 was removed from the environment by passing N_2 gas through the polymer solution for 5 min. As initiator, 2.5 mg of AIBN was dissolved in water and added to the solution and mixed until it became homogeneous. The solution (20 µL) was dripped onto the pre-allylated chip. The prepared SPR chips were placed under a UV lamb (100 W, 365 nm, Analytik Jena, Jena, Almanya) and polymerized by the photopolymerization reaction for 45 min. Unreacted monomers were removed with ethyl alcohol and dried in an oven. The NIP SPR chips were prepared in the same way without adding Neo to the polymer solution.

3.2.4. Template Removal Studies

The template molecule Neo was removed from the SPR chips using a 0.03 M NaCl solution. Neo-MIP SPR chip was placed in the SPR and washed with 0.03 M NaCl solution for 30 minutes, while the desorption solution was renewed every 10 minutes. Desorption continued until the ΔR value approached zero.

3.3. Characterization of SPR Chips

3.3.1. SEM Analysis

SEM analysis is used for morphology analysis of the synthesized nanofilm. First, 20 µl of polymer solution was dropped onto the SPR chip and coated with a spin coater. It was polymerized on the surface using a UV lamb. The nanofilm formed on the SPR chip was analyzed by SEM. For SEM analysis, the SPR chip was coated with gold and placed on the instrument plate. The SPR chips were analyzed with SEM (Quanta 650 Field Emission SEM, FEI) in Çukurova University Central Laboratory (ÇÜMERLAB). Images were taken from Neo-MIP and NIP SPR chips at different magnifications (50000x and 100000x).

3.3.2. FTIR Analysis

The SPR chips were characterized using the FTIR (FT/IR-6700, Jasco) instrument. For FTIR analysis, MIP and NIP nanofilms were synthesized and placed in the instrument in powder form. N_2 gas was introduced for 10 minutes to remove moisture and CO_2 from the measured sample chamber. The spectra obtained were recorded by scanning the wavenumber range (400-4000 cm-1).

3.3.3. Atomic Force Microscopy (AFM)

Characterization of the SPR chip atomic force photographed in semi-contact mode with a microscope (Park NX10, Park Systems). Due to its property as a free cantilever interferometer, the AFM can perform measurements at a very high resolution (4096 x 4096 pixels). The SPR chip was attached to the sample holder with double-sided adhesive tape. Imaging studies were performed in air in semi-contact mode. The vibrational resonance frequency (341.30 kHz) was applied. The vibration amplitude is 1 VRMS and the empty vibration amplitude is 2 VRMS. The samples were acquired as images of a (2 x 2 µm) area with a scanning speed of (2 µm/s) and a resolution of (256 x 256 pixels).

3.3.4. Contact angle measurements

The contact angle measurements were made using the Attension Theta, Biolin Scientific instrument. The contact angle was determined using the sessile drop method by dropping a drop of water onto the SPR chip. After water was dropped on different parts of the gold surfaces, 10 photos were taken and a separate contact angle was calculated for each photo. The device camera speed is 3009 FPS. The calculations use drop images of 1984 x 1264 pixels, which are critical to measurement accuracy.

The contact angle values obtained are the left contact angle taken from the left contact point of the drop with the solid; the right contact angle taken from the right contact point was obtained and the average contact angle values, which are the average of both points, were obtained. The average of the 10 contact angle values for the unmodified, Neo-MIP and NIP SPR chips was calculated.

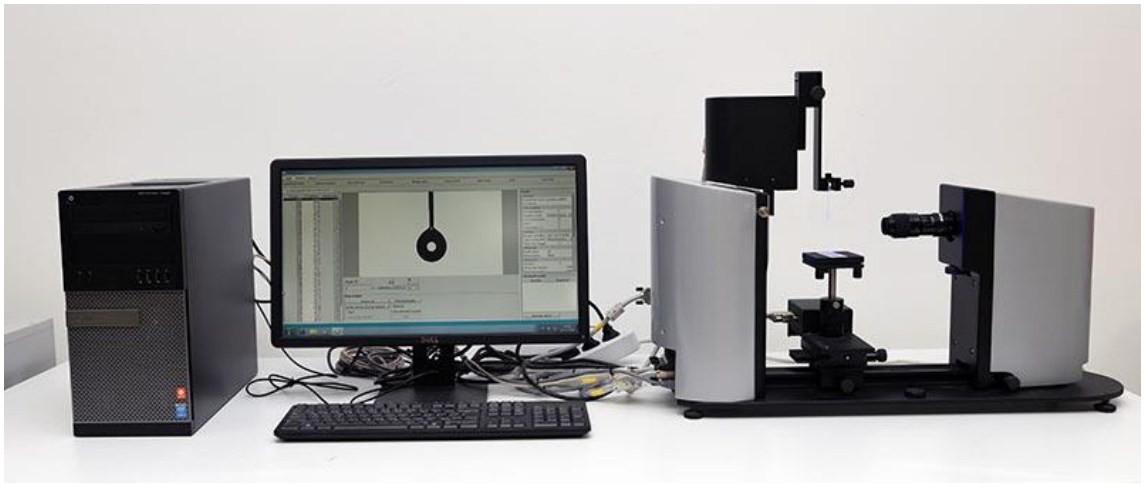

Figure 6. Contact angle device

3.4. Kinetic Analysis with Neo-MIP and NIP SPR Chips

Neo-MIP SPR chip was prepared using Neo as the template molecule and VIM as the functional monomer in the Neo-VIM precomplex. After Neo-MIP SPR chip was prepared, their kinetic studies were performed using Neo solutions at different concentrations (in the range of 3-50 ng/mL). First, the prepared chip was placed in the device and washed with ultrapure water (30 µl/min) until a stable peak was obtained. Then, Neo solutions in water at various concentrations (3, 4, 5, 10, 20, 30 and 50 ng/ml) were prepared and injected into the system one by one. It was applied for 30 minutes at a flow rate of 15 µL/min. The shift in resonance frequency was observed for each concentration due to Neo binding, and after reaching the equilibrium state, desorption was performed with 0.03 M NaCl solution (30 µL/min, 10 minutes, 25°C). After the desorption step, the SPR chip was washed again with ultrapure water. Calibration graph was created by using sensogram values of Neo concentrations at different concentrations. The SPRview software of the kinetic imaging program was used for the kinetic analysis studies.

3.5. Selectivity studies

The SPR chip, which has a Neo-specific cavity, was inserted into the SPR. It was then washed with water for 10 minutes. Neo and competitor molecules (pterin and glucose) solutions were prepared in water at the same concentration (20 ng/mL) and injected sequentially into the system for 30 min (15 µl/min). After reaching the equilibrium state, desorption was performed with 0.03 M NaCl solution for 10 min (30 µL/min, 25°C). Then, the SPR chip was washed again with ultrapure water. All processes were repeated for the NIP SPR chip.

3.6. Reusability

Neo solutions (20 ng/mL, 15 uL/min flow rate, 25°C) were fed to the SPR system 10 times and repeated to investigate the reusability of Neo-MIP SPR chips. In addition, the reusability was analyzed on different days to determine the shelf life of the SPR chips. Neo solution with a concentration of 20 ng/ml Neo was added to the SPR system, sensorgrams were recorded, and the efficiency of the SPR chips was determined.

3.7. Kinetic Analyzes From Natural Source

Human plasma from a natural source was used for the kinetic analysis studies. In this regard, samples from human serum (purchased from Sigma) were placed in EDTA-containing tubes and centrifuged at 3800 rpm for 30 minutes at room temperature to separate cells, filtered (3 μm Sartorius filter), and stored at -20 ˚C until use. Human plasma was melted at room temperature before use. Plasma samples diluted (1/20000) and spiked with different concentrations of Neo (5, 10, 20 and 50 ng/ml) were injected into the SPR system and sensorgrams were recorded. The same procedures used for the previous aqueous solution studies were used for the plasma studies.

4. RESULTS AND DISCUSSIONS

4.1. Preparation of Neo-VIM Precomplex

To investigate the effect of the amount of monomer used in the synthesis of the SPR chip on the amount of Neo adsorption, pre complexes with different molar ratios of Neo-VIM concentration (1:3, 1:4, 1:5, 1:6, 1:7) were prepared (Figure 7). According to the figure, the adsorption amount of Neo increased with the amount of monomers in the synthesis precomplex. Six different amounts of monomer were studied, and maximum Neo adsorption was achieved when the ratio of Neo-VIM was 1:5. When the ratio was changed to 1:6, there was not much difference. Therefore, the ideal molar ratio of 1:5 was assumed and applied in this study.

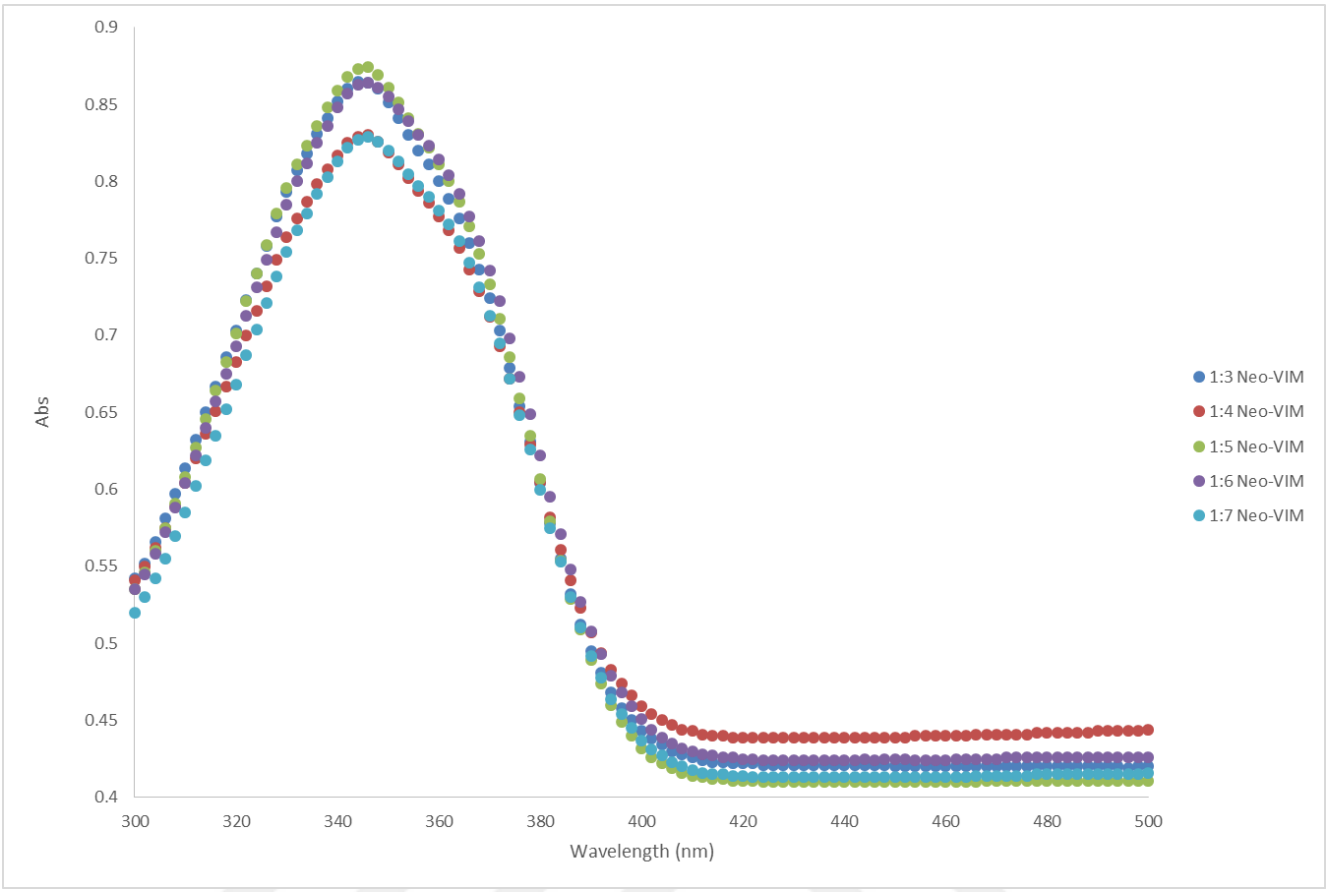

Figure 7. Spectrophotometric measurement of the Neo-VIM pre-complex

4.2. Characterization of Neo-MIP and NIP SPR Chips

4.2.1. SEM Images

The surface morphology of the Neo-MIP and NIP SPR chips was visualized using scanning electron microscope images (SEM). As shown in Figure 8, polymerization occurred homogeneously on the surface. SEM Photographs of Neo-MIP and NIP SPR chips were viewed at 50000X and 100000X magnification.

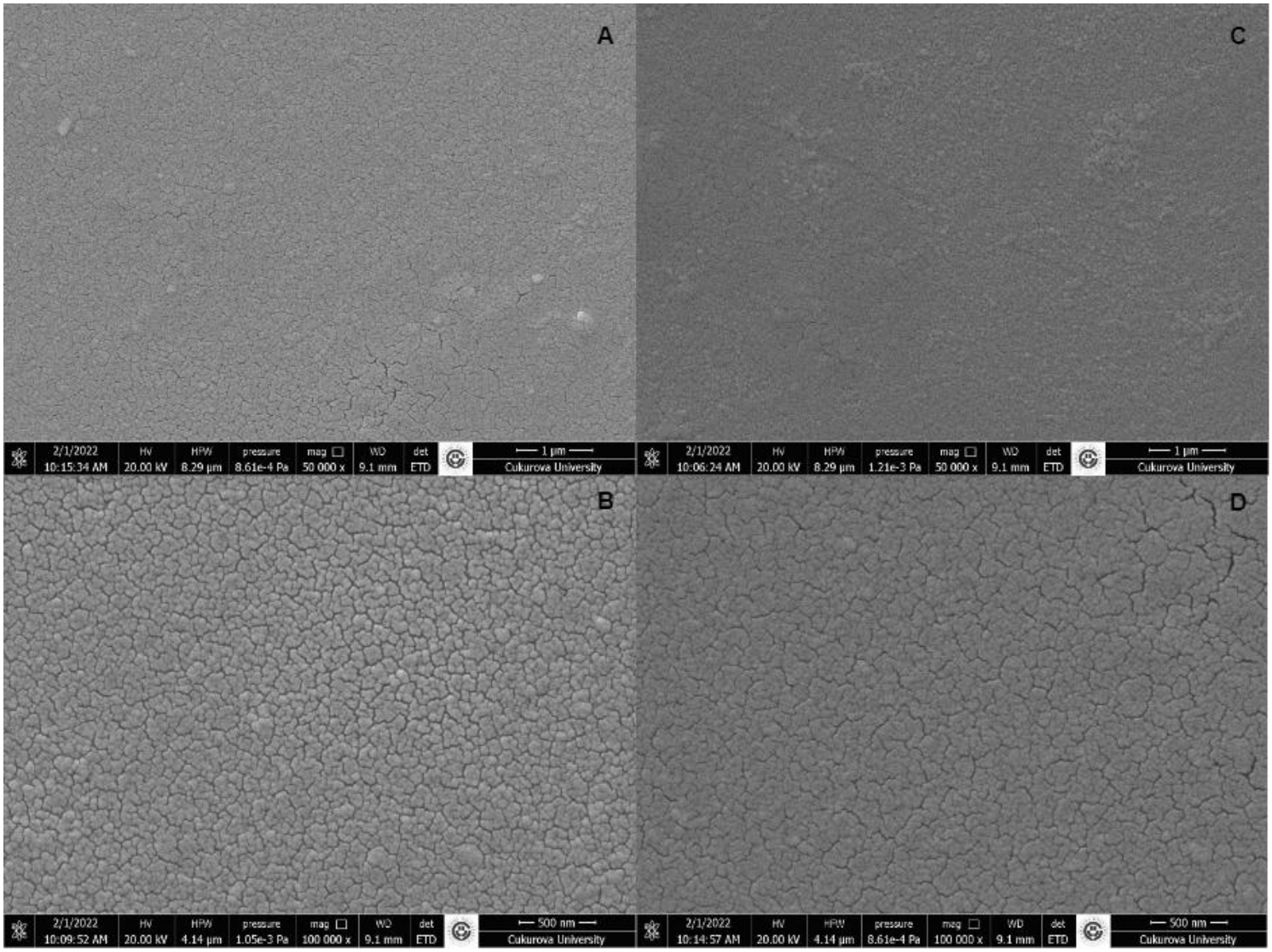

Figure 8. SEM Images A)Neo-MIP SPR chip (50000X), B) Neo-MIP SPR chip (100000X), C) NIP SPR chip (50000X), D)NIP SPR chip (100000X)

4.2.2. FTIR Analysis

An FTIR spectrophotometer (FT/IR -6700, Jasco) was used to characterize the SPR chips. The SPR chip was placed in the sample slot of the instrument and the total reflectance on the surface was measured in the wavenumber range 4000-400 cm-1. The FTIR spectrum of the Neo-MIP SPR chip is shown in Figure 9. The band formation at 602.65 and 811.88 cm-1 results from C-H bending vibrations in the precomplex and Neo-MIP structure. It can be said that the bands at 1104.05 cm-1 and 1263.15 cm-1 are caused by vibrations of aromatic and aliphatic double bonds (C=C, C=N) in the structure. Moreover, the frequency of the vibrational motion of the

N-H bending group has shifted from 1633 cm-1 to 1644.02 cm-1 (higher frequency). However, the frequency of the vibrational motions of the O-H and N-H stress groups has shifted from 3306 cm-1 to 3321.78 cm-1. These changes observed in the spectra indicate that Neo is involved in the structure.

In the spectrum of VIM, there is a clearly visible N-H stretching band in the range of 2820-3000 cm-1 and an O-H stretching band of the carboxylic acid at 3112 cm-1 (Daoud-Attieh M et al., 2013). When the FTIR spectrum of the precomplex of Neo-VIM is examined, a very broad peak is observed after complexation, which is due to the O-H stretching at 3300 cm-1. It can be said that the reason for the increase in the intensity of this peak and its shift to higher frequencies is due to the H-bonds formed by the complexation. Moreover, after complexation, the C=N stretching band shifted to the left and the peak in the C=N-C aromatic ring stretching band also increased in intensity and shifted to higher frequencies. Considering all these changes, it can be said that Neo and VIM successfully formed a preliminary complex.

The FTIR spectrum of the Neo-MIP SPR chip is shown in the Figure 9. Although the intense HEMA and EGDMA content in the structure covered the VIM and Neo molecules entering the structure, the existence of these molecules was successfully demonstrated. The O-H stress bands around 3404 cm-1 belong to the hydroxyl group of HEMA, which is abundant in the structure, the aliphatic C-H stress bands around 2950 cm-1 due to the methyl group in HEMA and EGDMA, the carbonyl group of EGDMA around 1720 cm-1, the C=O stretching bands of the double bond and the C-O stretching bands around 1130 cm-1 of EGDMA are seen in both spectra. When all the plots are examined, these changes in the spectra indicate that the Neo-VIM precomplex was incorporated into the structure of the Neo-MIP SPR chip.

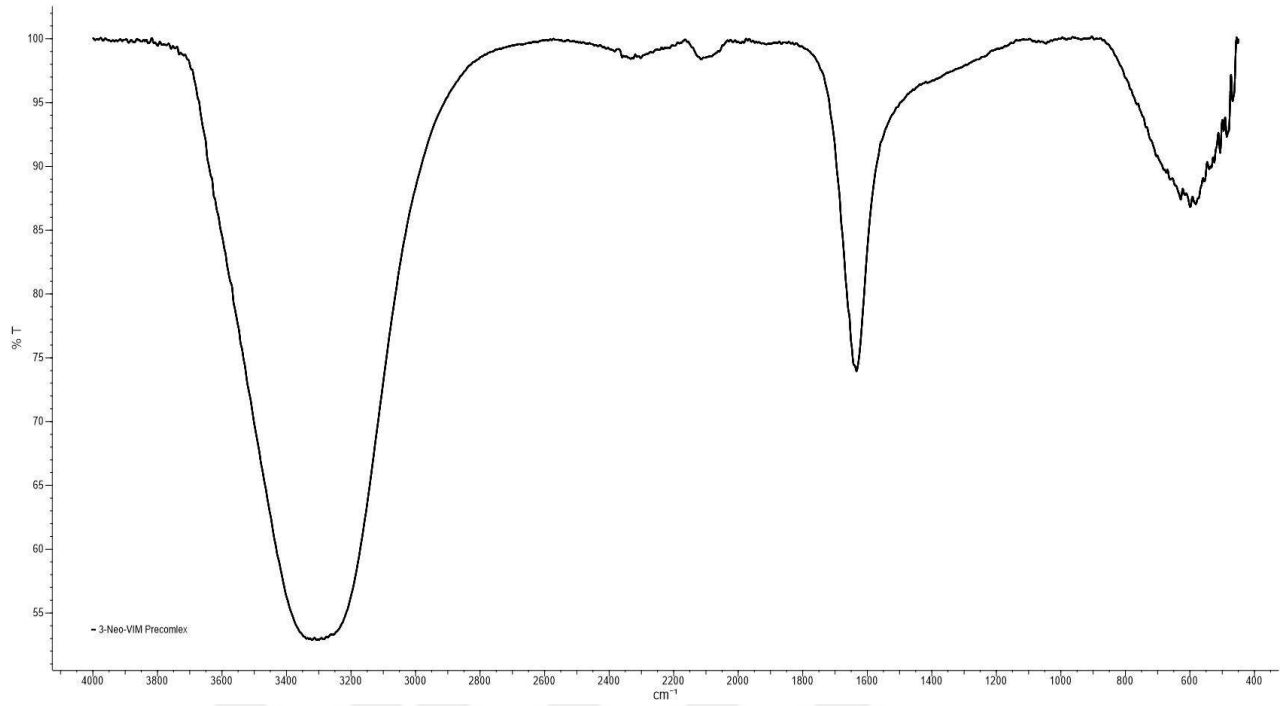

Figure 9. The FTIR spectra of Neo-VIM pre-complex

Figure 10. The FTIR spectra of Neo-MIP SPR chip

4.2.3. Atomic Force Microscopy (AFM)

The surface morphology of the unmodified and Neo-MIP SPR chips were characterized by atomic force microscopy in half-contact mode. The surface depth of the SPR sensor cleaned with acidic piranha solution was determined 6 nm and the surface depth of the Neo-MIP SPR chip was determined to be approximately 20 nm (Figure 11).

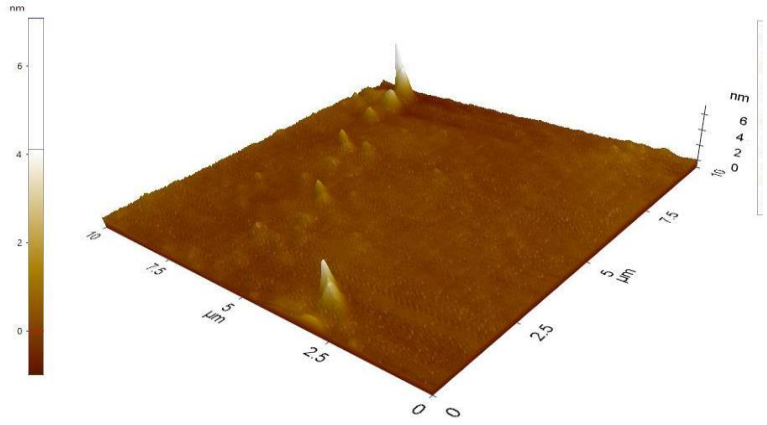

(A)

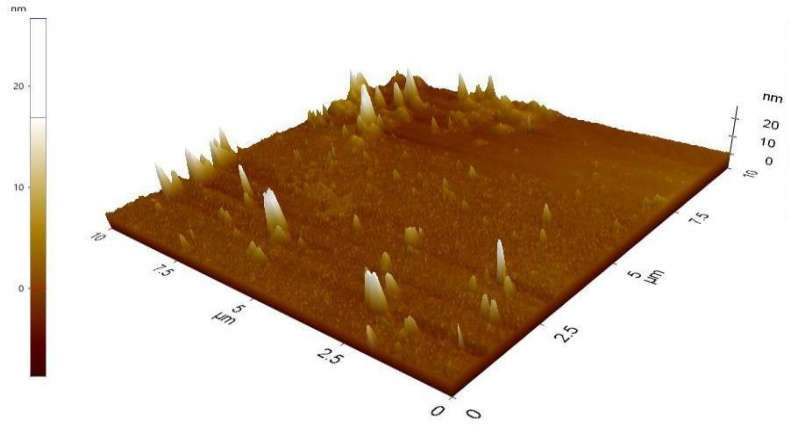

(B)

Figure 11. AFM Images (A) Unmodified chip, (B) Neo-MIP SPR chip

4.2.4. Contact angle measurements

Surface characterization of the unmodified SPR chip, Neo-MIP and NIP SPR chips were performed using Attension Theta, Biolin Scientific Contact Angle instrument. First, the chip is placed on the device with the nanofilm coated surface facing up and water is dripped onto it. Many measurements are taken from the right and left, and the contact angle value is calculated by averaging them. In contact angle measurement, water in contact with the solid surface creates a certain amount of angle. This angle varies depending on what the solid is in contact with, what the contacting liquid is, and it expresses the degree of wettability. The size of the contact angle depends on the size of the cohesion and adhesion forces. Table 2 summarizes the surface contact angles of the unmodified SPR chip, Neo-MIP and NIP SPR chips.

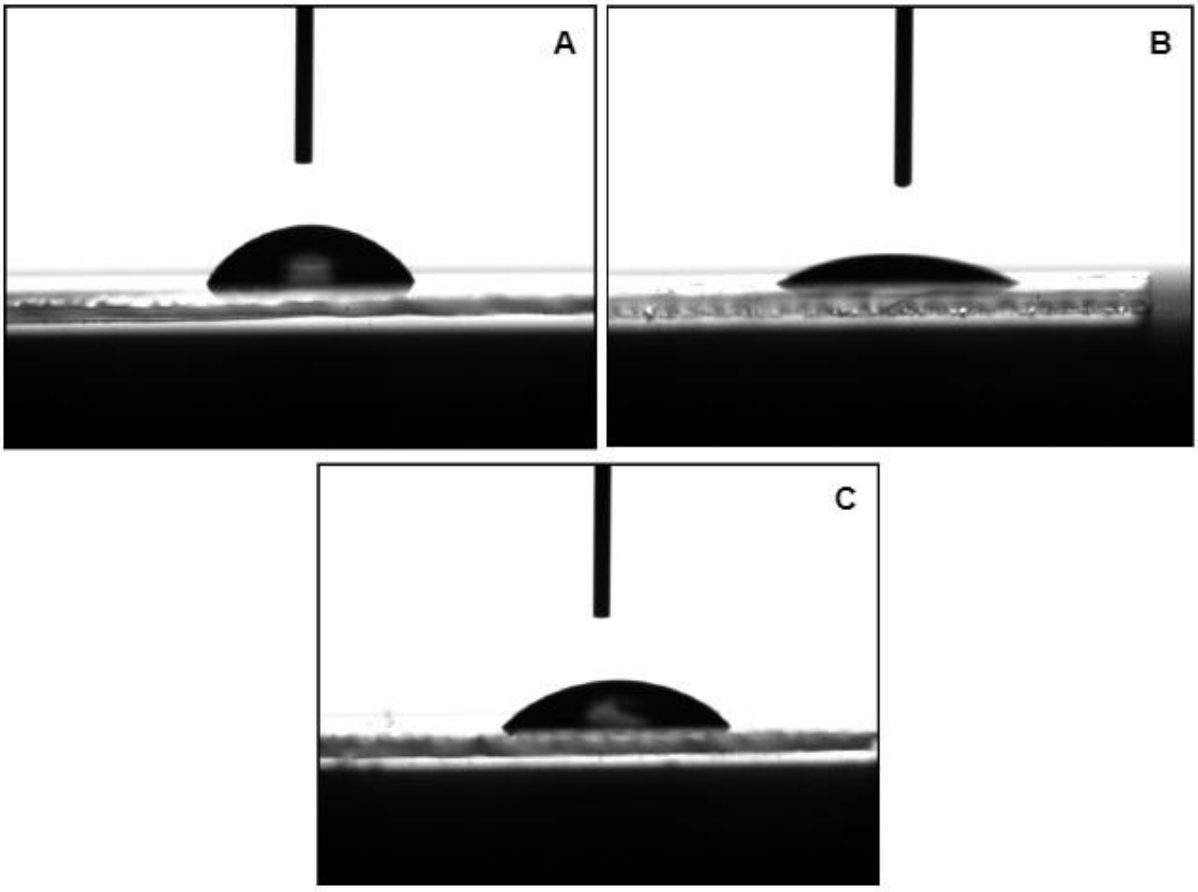

Figure 12. The contact angles of SPR chips A) Unmodified SPR chip, B) Neo-MIP SPR chip, C) NIP SPR chip

Table 2. The contact angles of surfaces

Surface	**Contact Angle, °**

Unmodified SPR chip	60.5
MIP SPR chip	32.7
NIP SPR chip	45.87

As can be seen from the contact angle measurements, the contact angle value 60.5 of the unmodified SPR chip surface decreased to 45.87 on the chip surface NIP SPR and to 32.7 after the Neo was imprinted. A significant decrease in the contact angle of the surface indicates that the hydrophilic property of the surface increases. This situation can be explained in two different ways; (i) HEMA was used as a functional monomer to form both imprinted and unimprinted nanofilm surfaces and it has a highly hydrophilic character. Therefore, attachment of a hydrophilic polymer to the surface increased the surface hydrophilicity and decreased the contact angle value.

(ii) The basic approach in this study is the formation of nanofilm surfaces on the chip surface. As a result of the MIP and NIP nanofilm layers formed on the surface, the roughness on the surface increases (See AFM results) and the increase in surface roughness increases the hydrophilicity of the surface. Due to the VIM and Neo content of the Neo-MIP SPR chip, it has a rougher surface than the NIP SPR chip. Therefore, the reduction in contact angle is greater than the NIP SPR chip. Contact angle images of unmodified Neo-MIP and NIP SPR chips for which contact angle measurements were taken are given in Figure 12.

4.3. Kinetic Analysis

4.3.1. Analysis of Neopterin Concentration

Unlike enzyme, radio, or fluorescent labeling methods that are commonly used in biomolecule determination, SPR-based biosensors can be used without any labeling (Homola, 2003). Eliminating labeling methods saves time and reduces costs. In addition, incorrect results can be obtained due to the interaction of label molecules with other molecules in the environment. These problems can be eliminated by using SPR-based biosensors. SPR-based MIP and NIP nanofilm biosensors can convert quantitative interactions into qualitative data by measuring changes in refractive index as a function of molecular interactions occurring on the sensor surface (Cooper et al., 2003).

In this study, a Neo-MIP SPR chip was prepared. Neo solutions were prepared at different concentrations (3, 4, 5, 10, 20, 30 and 50 ng/ml) to investigate the relationship between the SPR signal and Neo concentration. The solutions were interacted with the SPR chip via the peristaltic pump, and the kinetic data were obtained using the SPRview software. The sensorgrams obtained with different concentrations of Neo solutions are shown in Figure 13.

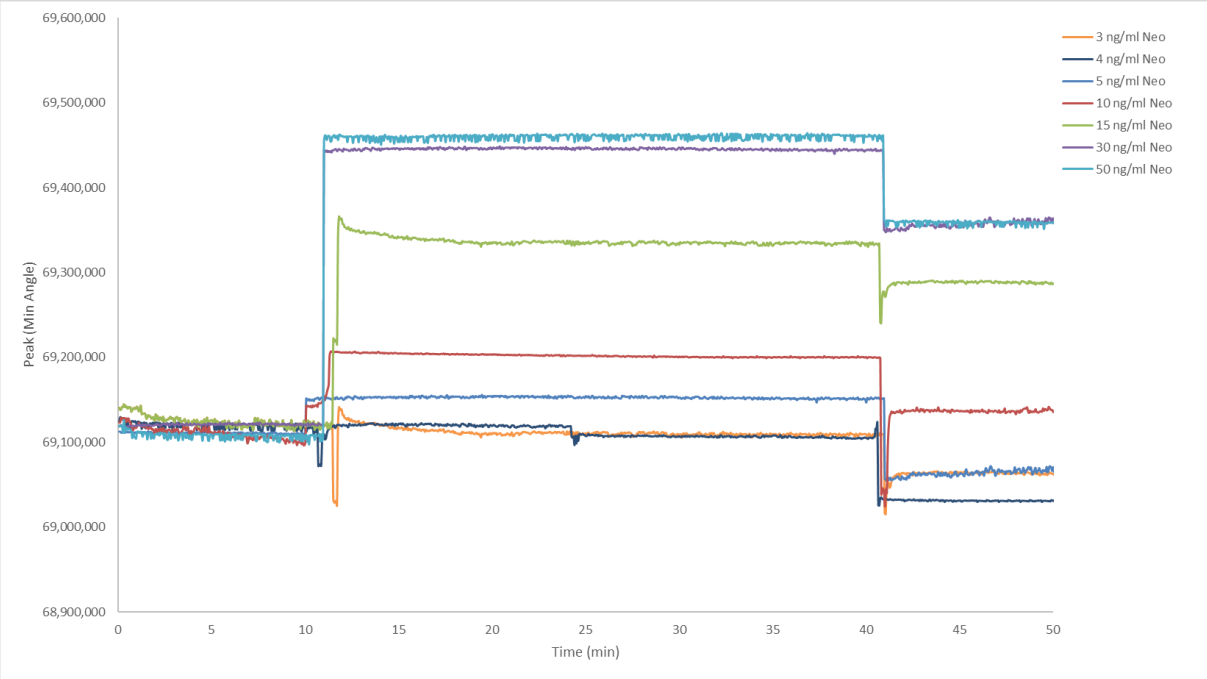

Figure 13. Sensograms obtained with different concentrations of Neo solutions

In the figure 13, the time-dependent change of the signal ΔR during the passage of the Neo molecule through the system is shown in the sensogram graph. As the Neo concentration increased, the SPR refractive index also increased. This means that the interaction of the analyte and the ligand has high affinity and selectivity.

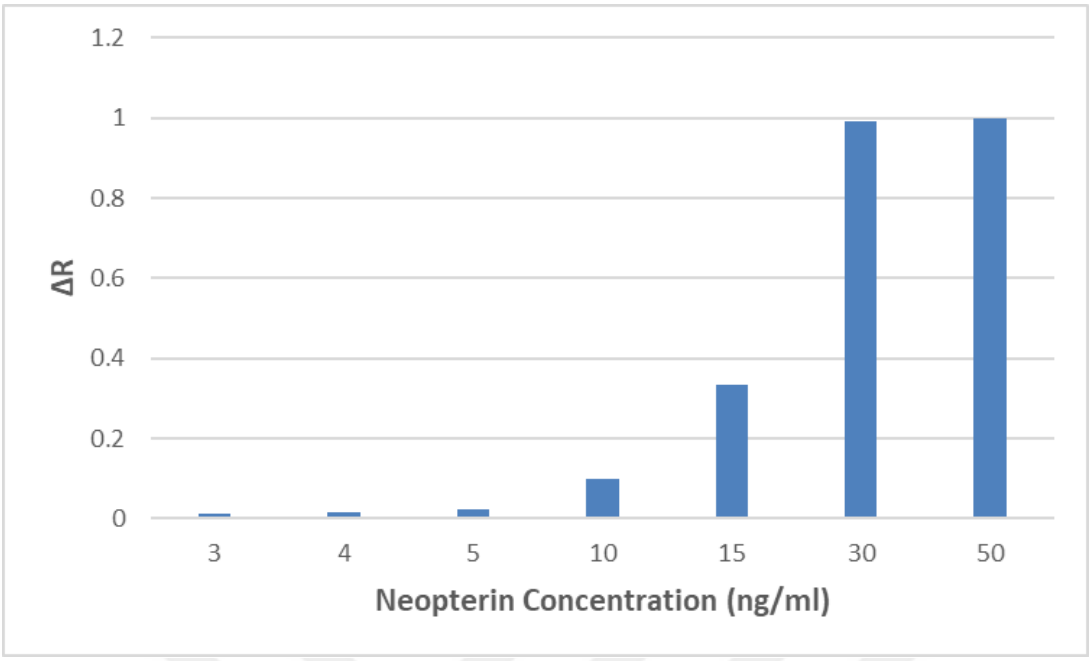

Figure 14. The relationship between Neo concentration and ΔR of the Neo-MIP SPR chip

4.3.2. Adsorption Isotherm Models

Three different models are used to determine the adsorption capacity.

1- Freundlich Model

The Freundlich model is used to determine the value of surface heterogeneity. It assumes that adhesion occurs through the formation of more than one adsorption layer.

$$\Delta R = \Delta R_{max} [C]\ 1/n \qquad \textbf{(Eq.2)}$$

In the model calculated using the equation, the heterogeneity index (1/n) varies between 0-1. The closer the heterogeneity index is to 1, the higher the homogeneity. At a value of 1, we can say that the system is homogeneous.

2- Langmuir Model

The Langmuir model is used to determine the value of surface homogeneity. It assumes that molecules attach to a fixed number of well-defined surfaces, each of which can hold only one molecule.

$$\Delta R = (\Delta R_{max} C)/(K_D+[C]) \quad \textbf{(Eq.3)}$$

3- Freundlich - Langmuir Model

The Langmuir-Freundlich model can be applied in systems for which Langmuir and Freundlich models are appropriate. This model is used to explain interactions on both heterogeneous and homogeneous surfaces.

$$\Delta R = \Delta R_{max}[C]1/n / K_D+[C]1/n \quad \textbf{(Eq.4)}$$

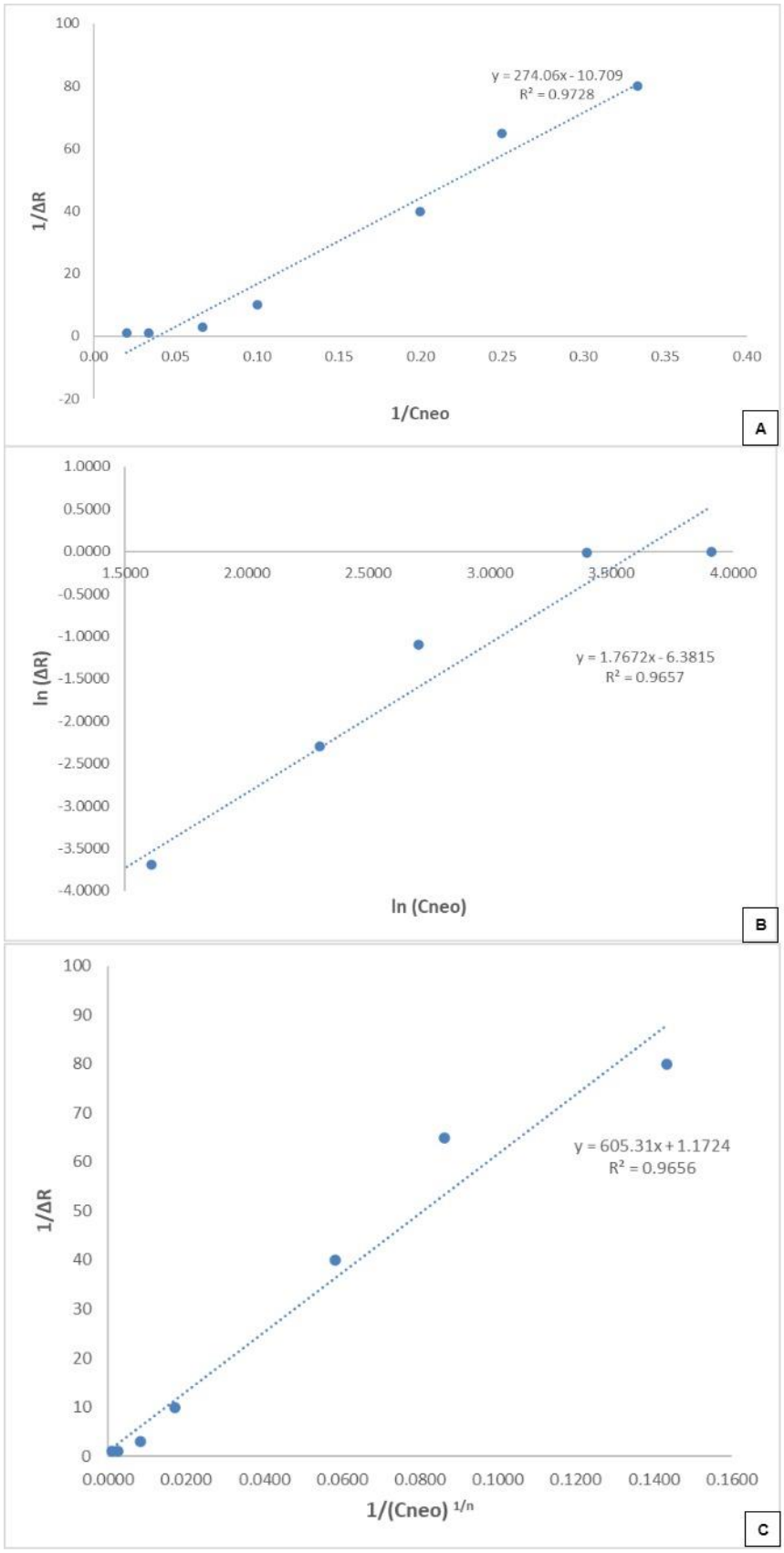

Figure 15. Adsorption models. A) Langmuir, B) Freundlich, C) Langmuir - Freundlich.

Table 3. Langmuir, Freundlich and Langmuir-Freundlich parameters

Langmuir		**Freundlich**		**Langmuir-Freundlich**	
ΔR_{max} (ng/mL)	0.0803	ΔR_{max} (ng/mL)	590.8133	ΔR_{max} (ng/mL)	0.8530
K_D (mL/ng)	23.7745	1/n	1.7672	1/n	1.7672
K_A (ng/mL)	0.0421	R^2	0.9657	K_D (mL/ng)	516.3
R^2	0.9728			K_A (ng/mL)	0.0019
				R^2	0.9656

According to Figure 15, the experimentally obtained data are mostly compatible with the Langmuir model (R^2 = 0.9728). This indicates that the Neo binding sites on the prepared imprinted sensor surface are homogeneously distributed, single-layered, equal in energy, and with minimal lateral interaction. The results of all three isotherm models are shown in Table 3.

4.4. Selectivity Studies

The most important feature of molecularly imprinted polymer-based SPR chips is the direct detection of the desired molecule without the need for a labeling step. Therefore, the quality of the prepared molecular imprinting is directly proportional to the selectivity of the sensor. The selectivity of the prepared molecularly imprinted sensors is calculated according to the selectivity coefficient and the imprinting selectivity coefficients.

The selectivity coefficient is calculated according to the formula below.

$$k = \Delta R_{template} / \Delta R_{competitor} \quad \textbf{(Eq.5)}$$

The imprinting selectivity coefficient is calculated with the following equation.

$$k' = k_{MIP} / k_{NIP} \quad \textbf{(Eq.6)}$$

In the study, MIP and NIP SPR chips were used for the selectivity studies of the nanofilm-based SPR sensor. Unlike the target molecule Neo, pterin and glucose were used as competitor molecules for selectivity control. 3 different molecules were passed through the SPR system in the form of suspensions prepared at a concentration of 15 ng/ml (Figure 11).

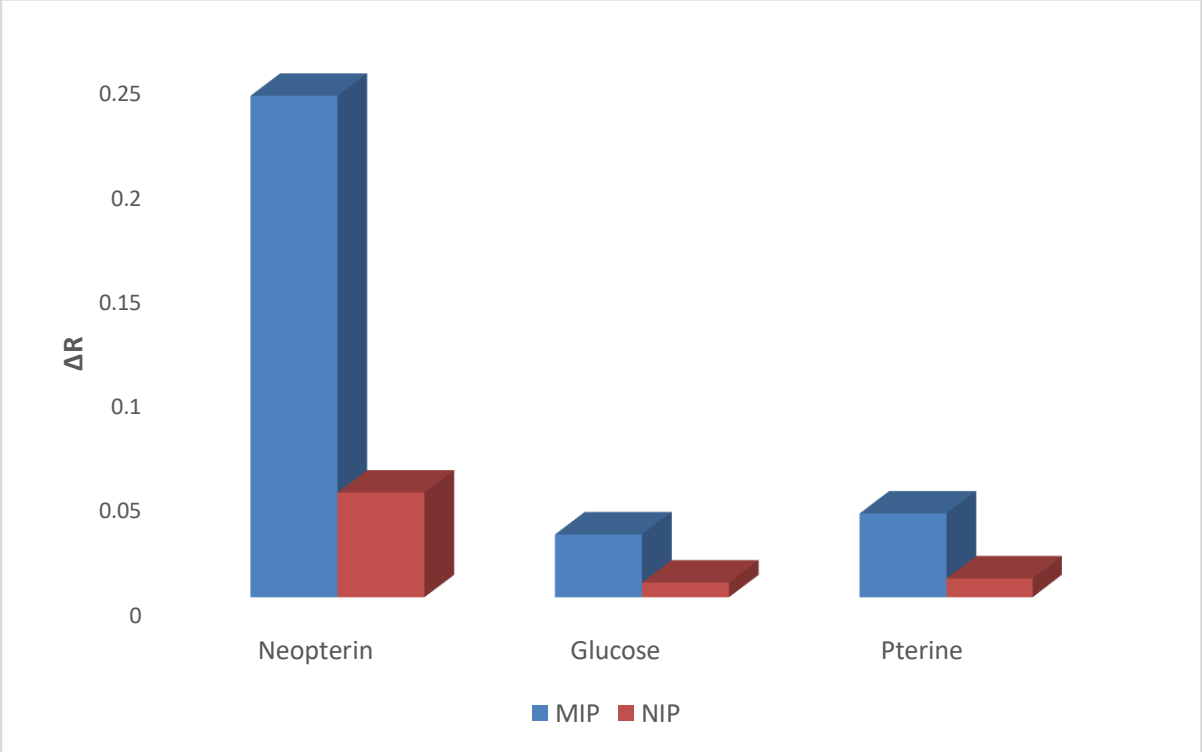

Figure 16. ΔR values of Neo, Pterin and Glucose competitor molecules (15 ng/ml) for interactions between Neo-MIP and NIP SPR chip

Table 4. Selectivity and relative selectivity coefficients for Neo with respect to Pterin and Glucose

	MIP		NIP		
Competitor Molecules	ΔR	K	ΔR	K	k´
Neo	0,33	-	0,05	-	-
Glucose	0,03	11	0,007	7.1429	1.54
Pterin	0,04	8,25	0,009	5.5556	1.485

4.5. Reusability Studies

To monitor the reuse of the Neo- MIP SPR chip, the figure shows the sensogram obtained by adding 15 ng/ml Neo solution to the sensor surface 10 times in succession. 0.03 M NaCl solution was used as the regeneration solution. It was found that 15 ng/ml Neo solution, when added to the system ten times in succession, can be reused without any visible change in the binding sites (Figure 17).

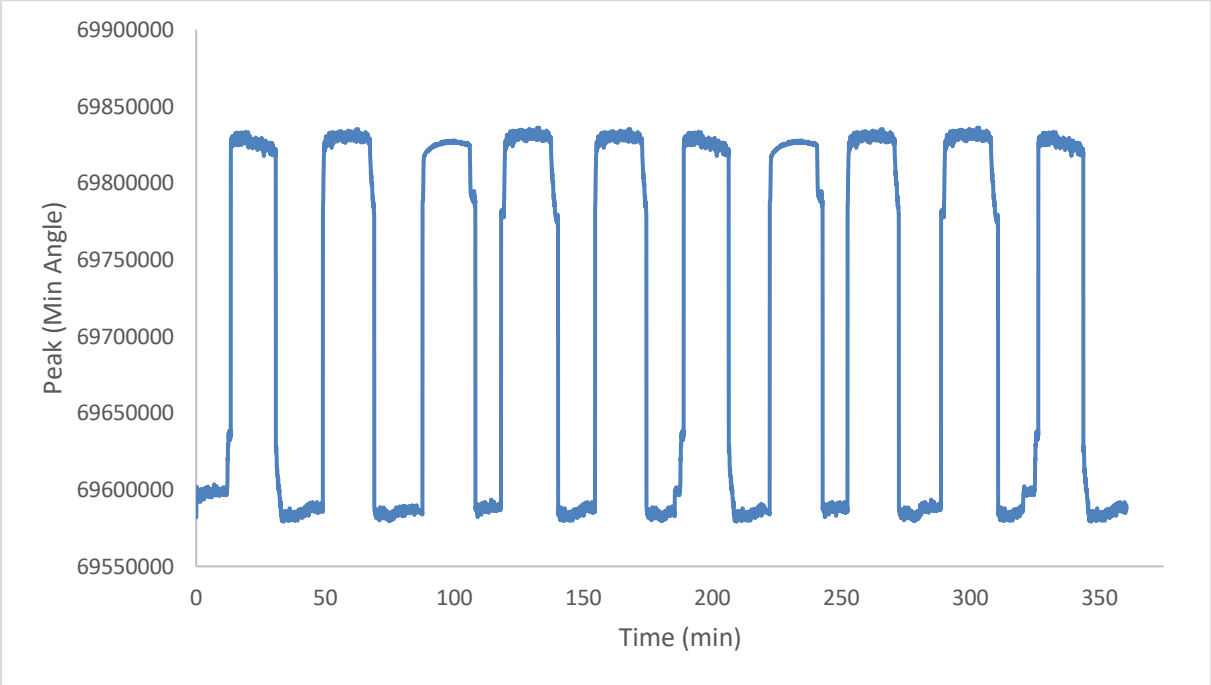

Figure 17. Reusability

4.6. Kinetic Analyzes From Natural Source

Neo-MIP SPR chip was used for the detection of Neo in human serum samples. Neo concentrations ranging from 5 ng/mL to 50 ng/mL were added to 1/20000 diluted plasma samples. In the analyzes performed with the Neo-MIP SPR chip, a change in peaks was observed in relation to the increase in Neo concentration. The sensogram curve of these samples is shown in Figure 18.

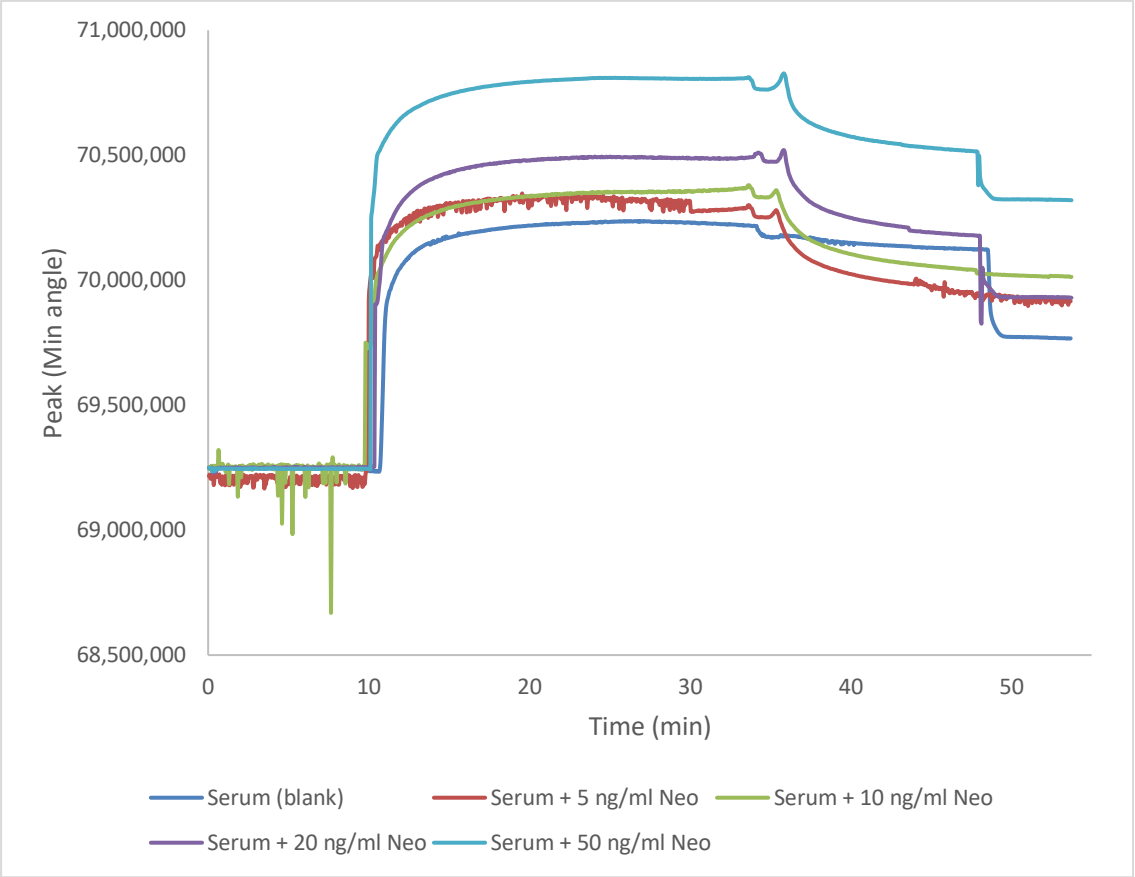

Figure 18. Sensograms of interactions between plasma and SPR chip.

In Figure 18, sensograms of time-varying peaks obtained from plasma studies are given. As seen in the figure, the signal value of the Neo-MIP SPR chip increases with decreasing dilution rate (increasing concentration). Even with a very high dilution rate (20000 times), the SPR chip appears to signal. The most important point of the results obtained from the experiments carried out in this context is the determination that Neo can be detected even in a complex environment such as plasma (91% water, 7% proteins, 2% ions, nutrients, gases, wastes, hormones). As a result; Neo-MIP SPR chips can be used successfully in the determination of Neo from both aqueous solutions and natural sources.

CONCLUSION

Since Neo increases with the activation of the immune system in the human body, it has become an important biomarker to be used in the early diagnosis of diseases. Therefore, in this study, studies aimed at detecting it with SPR were carried out. The nanofilm surface bonded to vinyl imidazole (VIM) was synthesized and its relationship with Neo was observed by experiments.

After the synthesized film was applied to the SPR chip, characterization studies were carried out with FTIR, AFM, SEM and contact angle. All the peaks to be observed in the polymerization were taken in FTIR. The contact angle and AFM results also confirmed the desired results about surface recognition, film thickness and distribution. Concentration change, selectivity and reproducibility were examined in kinetic studies, equilibrium analysis and isotherm results were analyzed. With the increase in concentration, the ΔR value increased. Equilibrium and binding analyses, on the other hand, showed that the binding was strong from a single region, as assumed, in line with the graphic results.

In particular, the Langmuir isotherm ΔR_{max}=0.0803 value is one step ahead of other isotherms, proving our sensor that the Neo binding is monolayer and homogeneous. In artificial plasma studies, it has been separated from other molecules that it can show affinity with, with a higher signal level, and its selectivity has been proven. In addition, the fact that the measurement can be made far below the previously emphasized clinical values proves the validity of the study. Finally, in reusability studies, it showed that it is a system suitable for reuse by giving signals with almost the same strength in 10 repeated experiments. Neo levels in humans are included in the literature as normal plasma values. Since it was shown in the experiments that clear and strong signals were obtained at concentrations between 3-50 ng/mL, the system proved that it could detect the Neo molecule with the desired sensitivity. It has been proven by the data that surface plasmon resonance sensors can be developed as an alternative to HPLC, fluorescence and electrochemical detection methods for the determination of Neo.

REFERENCES

Abate, G., Comella, Pasquale, Marfella, A., Santelli, G., Fiore, M., & Perna, M. (n.d.). *Prognostic Relevance of Urinary Neopterin in Non-Hodgkin's Lymphomas*. https://doi.org/10.1002/1097-0142

Akgönüllü, S., Yavuz, H., & Denizli, A. (2020). SPR nanosensor based on molecularly imprinted polymer film with gold nanoparticles for sensitive detection of aflatoxin B1. Talanta, 219, 121219

Altintas, Z. (n.d.). *Biosensors and nanotechnology : applications in health care diagnostics*. 382.

Altintas, Z., Uludag, Y., Gurbuz, Y., & Tothill, I. E. (2011). Surface plasmon resonance based immunosensor for the detection of the cancer biomarker carcinoembryonic antigen. *Talanta*, *86*(1), 377–383. https://doi.org/10.1016/J.TALANTA.2011.09.031

Andaç, M., Say, R., & Denizli, A. (2004). Molecular recognition based cadmium removal from human plasma. *Journal of Chromatography B*, *811*(2), 119–126. https://doi.org/10.1016/J.JCHROMB.2004.08.024

Bai, H., Wang, R., Hargis, B., Lu, H., & Li, Y. (2012a). A SPR aptasensor for detection of avian influenza virus H5N1. *Sensors (Basel, Switzerland)*, *12*(9), 12506–12518. https://doi.org/10.3390/S120912506

Beigel, J. (2005). The emerging utility of Neopterin? In *Clinical Immunology* (Vol. 116, Issue 1). https://doi.org/10.1016/j.clim.2005.03.008

Berdowska, A., & Zwirska-Korczala, K. (2001a). Neopterin measurement in clinical diagnosis. *Journal of Clinical Pharmacy and Therapeutics*, *26*(5), 319–329. https://doi.org/10.1046/J.1365-2710.2001.00358.X

Bereli, N., Çimen, D., & Denizli, A. (2021). Optical sensor-based molecular imprinted poly (hydroxyethyl methacrylate-N-methacryloyl-(L)-histidine methyl ester) thin films for determination of tartrazine in fruit juice. IEEE Sensors Journal, 21(12), 13215-13222.

Biacore. (n.d.). *GE Healthcare Biacore Sensor Surface Handbook*.

Bichler, A., Fuchs, D., Hausen, A., Hetzel, H., Reibnegger, G., & Wachter, H. (1983). Measurement of urinary Neopterin in normal pregnant and non-pregnant women and in women with benign and malignant genital tract neoplasms. *Archives of Gynecology*, *233*(2), 121–130. https://doi.org/10.1007/BF02114788

Budavari, S. (1989). The Merck index : an encyclopedia of chemicals, drugs, and biologicals. In *The Merck Index* (Vol. 1174). Merck.

Bührer-Sekula, S., Hamerlinck, F. F. V., Out, T. A., Bordewijk, L. G., & Klatser, P. R. (2000). Simple dipstick assay for semi-quantitative detection of Neopterin in sera. *Journal of Immunological Methods*, *238*(1–2). https://doi.org/10.1016/S0022-1759(00)00148-4

Çaksen, H., Üstünbaş, H. B., & Çiftçi, A. (1998a). Neopterin ve Klinik Tanıdaki Önemi . *Neopterin ve Klinik Tanıdaki Önemi* , 206–213.

Caygill, R. L., Blair, G. E., & Millner, P. A. (2010). A review on viral biosensors to detect human pathogens. *Analytica Chimica Acta*, *681*(1–2), 8–15. https://doi.org/10.1016/J.ACA.2010.09.038

Centi, S., Tombelli, S., Puntoni, M., Domenici, C., Franek, M., & Palchetti, I. (2015). Detection of biomarkers for inflammatory diseases by an electrochemical immunoassay: The case of Neopterin. *Talanta*, *134*. https://doi.org/10.1016/j.talanta.2014.10.053

Chang, Y. F., Wang, W. H., Hong, Y. W., Yuan, R. Y., Chen, K. H., Huang, Y. W., Lu, P. L., Chen, Y. H., Chen, Y. M. A., Su, L. C., & Wang, S. F. (2018). Simple Strategy for Rapid and Sensitive Detection of Avian Influenza A H7N9 Virus Based on Intensity-Modulated SPR Biosensor and New Generated Antibody. *Analytical Chemistry*, *90*(3), 1861–1869. https://doi.org/10.1021/ACS.ANALCHEM.7B03934

Chavanieu, A., & Pugnière, M. (2016). Developments in SPR Fragment Screening. *Expert Opinion on Drug Discovery*, *11*(5), 489–499. https://doi.org/10.1517/17460441.2016.1160888

Cooper, M. A. (2003). Label-free screening of bio-molecular interactions. *Analytical and Bioanalytical Chemistry*, *377*(5), 834–842. https://doi.org/10.1007/S00216-003-2111-Y/FIGURES/7

Cormack, P. A. G., & Mosbach, K. (1999). Molecular imprinting: Recent developments and the road ahead. *Reactive and Functional Polymers*, *41*(1), 115–124. https://doi.org/10.1016/S1381-5148(99)00024-3

Dastmalchi, B., Tassin, P., Koschny, T., Soukoulis, C. M., Dastmalchi, B., Koschny, T., & Soukoulis, C. M. (2016). A New Perspective on Plasmonics: Confinement and Propagation Length of Surface Plasmons for Different Materials and Geometries. *Advanced Optical Materials*, *4*(1), 177–184. https://doi.org/10.1002/ADOM.201500446

de Castro, M. R., di Marco, G. S., Arita, D. Y., Teixeira, L. C., Pereira, A. B., & Casarini, D. E. (2004). Urinary Neopterin quantification by reverse-phase high-performance liquid chromatography with ultraviolet detection. *Journal of Biochemical and Biophysical Methods*, *59*(3), 275–283. https://doi.org/10.1016/J.JBBM.2004.03.004

Denz, H., Fuchs, D., Huber, H., Nachbaur, D., Reibnegger, G., Thaler, J., Werner, E. R., & Wachter, H. (1990). Correlation between Neopterin, interferon-gamma and haemoglobin in

patients with haematological disorders. *European Journal of Haematology*, *44*(3), 186–189. https://doi.org/10.1111/J.1600-0609.1990.TB00374.X

Durukan, A. H., Hürmeriç, V., Akgül, E. Ö., Erdem, Ü., Kiliç, S., Erbil, K., & Bayraktar, M. Z. (2004). Üveitli olgularda idrar Neopterin seviyesi ile hastalık aktivitesi arasındaki ilişkinin değerlendirilmesi. *Üveitli Olgularda Idrar Neopterin Seviyesi Ile Hastalık Aktivitesi Arasındaki Ilişkinin Değerlendirilmesi*, 238–242. https://app.trdizin.gov.tr/publication/paper/detail/TlRJeU1qUTA

Erganiş, O., & İstanbulluoğlu, E. (1993a). *İmmünoloji* .

Erickson, D., Mandal, S., Yang, A. H. J., & Cordovez, B. (2008). Nanobiosensors: Optofluidic, electrical and mechanical approaches to biomolecular detection at the nanoscale. *Microfluidics and Nanofluidics*, *4*(1–2), 33–52. https://doi.org/10.1007/S10404-007-0198-8/FIGURES/7

Ersöz, A., Say, R., & Denizli, A. (2004). Ni(II) ion-imprinted solid-phase extraction and preconcentration in aqueous solutions by packed-bed columns. *Analytica Chimica Acta*, *502*(1), 91–97. https://doi.org/10.1016/J.ACA.2003.09.059

Fano, U. (1941). The Theory of Anomalous Diffraction Gratings and of Quasi-Stationary Waves on Metallic Surfaces (Sommerfeld's Waves). *JOSA, Vol. 31, Issue 3, Pp. 213-222*, *31*(3), 213–222. https://doi.org/10.1364/JOSA.31.000213

Farka, Z., Juřík, T., Pastucha, M., & Skládal, P. (2016). Enzymatic Precipitation Enhanced Surface Plasmon Resonance Immunosensor for the Detection of Salmonella in Powdered Milk. *Analytical Chemistry*, *88*(23), 11830–11836. https://doi.org/10.1021/ACS.ANALCHEM.6B03511

Fuchs, D., Stahl-Hennig, C., Gruber, A., Murr, C., Hunsmann, G., & Wachter, H. (1994). *Neopterin--its clinical use in urinalysis*. https://pubmed.ncbi.nlm.nih.gov/7869677/

Fuchs, D., Weiss, G., Reibnegger, G., & Wachter, H. (1992). The role of Neopterin as a monitor of cellular immune activation in transplantation, inflammatory, infectious, and malignant diseases. *Critical Reviews in Clinical Laboratory Sciences*, *29*(3–4), 307–344. https://doi.org/10.3109/10408369209114604

Ge, Y., Wu, B., Qi, X., Zhao, K., Guo, X., Zhu, Y., Qi, Y., Shi, Z., Zhou, M., Wang, H., & Cui, L. (2013). Rapid and sensitive detection of novel avian-origin influenza A (H7N9) virus by reverse transcription loop-mediated isothermal amplification combined with a lateral-flow device. *PloS One*, *8*(8). https://doi.org/10.1371/JOURNAL.PONE.0069941

Gieseg, S. P., & Cato, S. (2003). Inhibition of THP-1 cell-mediated low-density lipoprotein oxidation by the macrophage-synthesised pterin, 7,8-dihydroNeopterin. *Redox Report*, *8*(2). https://doi.org/10.1179/135100003125001396

Hall, A. J., Emgenbroich, M., & Sellergren, B. (2005). Imprinted Polymers. *Topics in Current Chemistry*, *249*, 317–349. https://doi.org/10.1007/B104333

Hamerlinck, F. F. V. (1999). Neopterin: A review. In *Experimental Dermatology* (Vol. 8, Issue 3). https://doi.org/10.1111/j.1600-0625.1999.tb00367.x

Hammerer-Lercher, A., Puschendorf, B., Fuchs, D., Mair, J., Tews, G., Shebl, O., & Sommer, R. (2006). Possible placental exchange of Neopterin as indicated by significant correlations in matched maternal neonatal blood samples at delivery [1]. In *Clinica Chimica Acta* (Vol. 365, Issues 1–2). https://doi.org/10.1016/j.cca.2005.08.002

Haupt, K. (2003). Molecularly imprinted polymers: the next generation. *Analytical Chemistry*, *75*(17), 376 A-383 A. https://doi.org/10.1021/AC031385H

Helmerhorst, E., Chandler, D. J., Nussio, M., & Mamotte, C. D. (n.d.). *Real-time and Label-free Bio-sensing of Molecular Interactions by Surface Plasmon Resonance: A Laboratory Medicine Perspective. | Semantic Scholar*. Retrieved June 30, 2022, from https://www.semanticscholar.org/paper/Real-time-and-Label-free-Bio-sensing-of-Molecular-A-Helmerhorst-Chandler/ff80716b5d39041338739cd3343d1f9176e69ba2

Hoffmann, G., Wirleitner, B., & Fuchs, D. (2003). Potential role of immune system activation-associated production of Neopterin derivatives in humans. In *Inflammation Research* (Vol. 52, Issue 8). https://doi.org/10.1007/s00011-003-1181-9

Homola, J. (2003). Present and future of surface plasmon resonance biosensors. *Analytical and Bioanalytical Chemistry*, *377*(3), 528–539. https://doi.org/10.1007/S00216-003-2101-0

Homola, J. (2006). *Surface Plasmon Resonance Based Sensors*. *4*. https://doi.org/10.1007/B100321

Homola, J. (2008). Surface plasmon resonance sensors for detection of chemical and biological species. *Chemical Reviews*, *108*(2), 462–493. https://doi.org/10.1021/CR068107D/ASSET/CR068107D.FP.PNG_V03

Horak, E., Gassner, I., Sölder, B., Wachter, H., & Fuchs, D. (1998). Neopterin levels and pulmonary tuberculosis in infants. *Lung*, *176*(5), 337–344. https://doi.org/10.1007/PL00007615

Huang, C. Y., Hsieh, C. H., Chen, Y. L., Lee, M. H., Lin, C. F., Tsai, H. H., Juang, Y. Z., Liu, B. D., & Lin, H. Y. (2011). Portable potentiostatic sensor integrated with Neopterin-imprinted poly(ethylene-co-vinyl alcohol)-based electrode. *IET Nanobiotechnology*, *5*(4), 126–131. https://doi.org/10.1049/IET-NBT.2011.0020

Huber, C., Richard Batchelor, J., Fuchs, D., Hausen, A., Lang, A., Niederwieser, D., Reibnegger, G., Swetly, P., Troppmair, J., & Wachter, H. (1984). Immune response-associated

production of Neopterin: Release from macrophages primarily under control of interferon-gamma. *Journal of Experimental Medicine*, *160*(1). https://doi.org/10.1084/jem.160.1.310

Hyland, K., & Howells, D. W. (1988). Analysis and clinical significance of pterins. *Journal of Chromatography*, *429*(C), 95–121. https://doi.org/10.1016/S0378-4347(00)83868-2

Jena, S. C., Shrivastava, S., Saxena, S., Kumar, N., Maiti, S. K., Mishra, B. P., & Singh, R. K. (2019). Surface plasmon resonance immunosensor for label-free detection of BIRC5 biomarker in spontaneously occurring canine mammary tumours. *Scientific Reports 2019 9:1*, *9*(1), 1–12. https://doi.org/10.1038/s41598-019-49998-x

Justino, C., Rocha-Santos, T., Analytical, A. D.-T. T. in, & 2010, undefined. (n.d.). Review of analytical figures of merit of sensors and biosensors in clinical applications. *Elsevier*. Retrieved April 3, 2022, from https://www.sciencedirect.com/science/article/pii/S0165993610002141?casa_token=BSg1O4Kzng8AAAAA:QQ4UAWJthzmvJQ0uQoTXm6cnllVItRCJbj6klAfSyTTS1jcbChtnkqtGZJ4jO5PeLX47HLOqVfA

Khoo, W. C., Kamaruzaman, S., Lim, H. N., Jamil, S. N. A. M., & Yahaya, N. (2019). Synthesis and characterization of graphene oxide-molecularly imprinted polymer for Neopterin adsorption study. *Journal of Polymer Research*, *26*(8). https://doi.org/10.1007/S10965-019-1847-9

Kihm, K. D., Cheon, S., Park, J. S., Kim, H. J., Lee, J. S., Kim, I. T., & Yi, H. J. (2012). Surface plasmon resonance (SPR) reflectance imaging: Far-field recognition of near-field phenomena. *Optics and Lasers in Engineering*, *50*(1), 64–73. https://doi.org/10.1016/J.OPTLASENG.2011.07.003

Komiyama, M. (2003). *Molecular imprinting : from fundamentals to applications*. 147.

Kretschmann, E., & Raether, H. (1968). Radiative Decay of Non Radiative Surface Plasmons Excited by Light. *Zeitschrift Fur Naturforschung - Section A Journal of Physical Sciences*, *23*(12), 2135–2136. https://doi.org/10.1515/ZNA-1968-1247/MACHINEREADABLECITATION/RIS

Liedberg, B., Nylander, C., & Lunström, I. (1983a). Surface plasmon resonance for gas detection and biosensing. *Sensors and Actuators*, *4*(C), 299–304. https://doi.org/10.1016/0250-6874(83)85036-7

Mahony, J. O., Nolan, K., Smyth, M. R., & Mizaikoff, B. (2005). Molecularly imprinted polymers—potential and challenges in analytical chemistry. *Analytica Chimica Acta*, *534*(1), 31–39. https://doi.org/10.1016/J.ACA.2004.07.043

Maier, S. A. (2007). Plasmonics: Fundamentals and applications. *Plasmonics: Fundamentals and Applications*, 1–223. https://doi.org/10.1007/0-387-37825-1

Malitesta, C., Mazzotta, E., Picca, R. A., Poma, A., Chianella, I., & Piletsky, S. A. (2012). MIP sensors - The electrochemical approach. In *Analytical and Bioanalytical Chemistry* (Vol. 402, Issue 5). https://doi.org/10.1007/s00216-011-5405-5

Mijangos, I., Navarro-Villoslada, F., Guerreiro, A., Piletska, E., Chianella, I., Karim, K., Turner, A., & Piletsky, S. (2006). Influence of initiator and different polymerisation conditions on performance of molecularly imprinted polymers. *Biosensors and Bioelectronics*, *22*(3), 381–387. https://doi.org/10.1016/J.BIOS.2006.05.012

Mosbach, K., & Ramström, O. (1996). The Emerging Technique of Molecular Imprinting and Its Future Impact on Biotechnology. *Bio/Technology 1996 14:2*, *14*(2), 163–170. https://doi.org/10.1038/nbt0296-163

Müftüoğlu, E., Bolaman, Z., Bilgir, O., & Ertop, S. (1993a). *İmmünoloji* .

Mujahid, A., & Dickert, F. L. (2016). Molecularly Imprinted Polymers: Principle, Design, and Enzyme-Like Catalysis. *Molecularly Imprinted Catalysts: Principles, Syntheses, and Applications*, 79–101. https://doi.org/10.1016/B978-0-12-801301-4.00005-0

Müller, M. M., Curtius, H. C., Herold, M., & Huber, C. H. (1991). Neopterin in clinical practice. In *Clinica Chimica Acta* (Vol. 201, Issues 1–2). https://doi.org/10.1016/0009-8981(91)90019-9

Müller, T. F., Vogl, M., Neumann, M. C., Lange, H., Grimm, M., & Müller, M. M. (1998). Noninvasive monitoring using serum amyloid A and serum Neopterin in cardiac transplantation. *Clinica Chimica Acta; International Journal of Clinical Chemistry*, *276*(1), 63–74. https://doi.org/10.1016/S0009-8981(98)00100-4

Neopterin excretion after liver transplantation and its value in differential diagnosis of complications. (n.d.). Retrieved May 16, 2022, from https://pubmed.ncbi.nlm.nih.gov/2552627/

Nguyen, V. T., Seo, H. bin, Kim, B. C., Kim, S. K., Song, C. S., & Gu, M. B. (2016). Highly sensitive sandwich-type SPR based detection of whole H5Nx viruses using a pair of aptamers. *Biosensors & Bioelectronics*, *86*, 293–300. https://doi.org/10.1016/J.BIOS.2016.06.064

Nichol, C. A., Smith, G. K., & Duch, D. S. (1985). Biosynthesis and metabolism of tetrahydrobiopterin and molybdopterin. In *Annual Review of Biochemistry: Vol. VOL. 54*. https://doi.org/10.1146/annurev.biochem.54.1.729

Oliveira, M. D. L., de Melo, C. P., Oliva, G., & Andrade, C. A. S. (2011a). Development of impedimetric and optical calcium biosensor by using modified gold electrode with porcine S100A12 protein. *Colloids and Surfaces. B, Biointerfaces*, *82*(2), 365–370. https://doi.org/10.1016/J.COLSURFB.2010.09.019

Omar, N. A. S., Fen, Y. W., Abdullah, J., Mustapha Kamil, Y., Daniyal, W. M. E. M. M., Sadrolhosseini, A. R., & Mahdi, M. A. (2020). Sensitive Detection of Dengue Virus Type 2 E-Proteins Signals Using Self-Assembled Monolayers/Reduced Graphene Oxide-PAMAM Dendrimer Thin Film-SPR Optical Sensor. *Scientific Reports*, *10*(1). https://doi.org/10.1038/S41598-020-59388-3

Ormazabal, A., García-Cazorla, A., Fernández, Y., Fernández-Álvarez, E., Campistol, J., & Artuch, R. (2005). HPLC with electrochemical and fluorescence detection procedures for the diagnosis of inborn errors of biogenic amines and pterins. *Journal of Neuroscience Methods*, *142*(1), 153–158. https://doi.org/10.1016/j.jneumeth.2004.08.007

Otto, A. (1968a). Excitation of nonradiative surface plasma waves in silver by the method of frustrated total reflection. *Zeitschrift Für Physik A Hadrons and Nuclei 1968 216:4*, *216*(4), 398–410. https://doi.org/10.1007/BF01391532

Ozgur Akgul, E., Aydın, İ., Caycı, T., Gulcan Kurt, Y., Nuri Aydın, F., & Agıllı, M. (n.d.). *The indicator of cellular immune response in body fluids: Neopterin*. https://doi.org/10.5455/gulhane.39000

Ozmeriç, N., Baydar, T., Bodur, A., Engin, A. B., Uraz, A., Eren, K., & Sahin, G. (2002). Level of Neopterin, a marker of immune cell activation in gingival crevicular fluid, saliva, and urine in patients with aggressive periodontitis. *Journal of Periodontology*, *73*(7), 720–725. https://doi.org/10.1902/JOP.2002.73.7.720

Park, K., Lee, J. M., Jung, Y., Habtemariam, T., Salah, A. W., Fermin, C. D., & Kim, M. (2011a). Combination of cysteine- and oligomerization domain-mediated protein immobilization on a surface plasmon resonance (SPR) gold chip surface. *Analyst*, *136*(12), 2506–2511. https://doi.org/10.1039/C0AN00966K

Pichler, R., Berg, J., Maschek, W., Schimetta, W., Steinwender, C., Hofmann, R., & Leisch, F. (2004). Proinflammatory parameters as CRP and IL-6 do not discriminate between post-PCI cardiac patients with and without exercise-induced ischemia as indicated by Tl-201 myocardial scintigraphy. *Cardiovascular Pathology : The Official Journal of the Society for Cardiovascular Pathology*, *13*(6), 299–305. https://doi.org/10.1016/J.CARPATH.2004.08.001

Piletsky, S. A., Piletskaya, E. v., Panasyuk, T. L., El'skaya, A. v., Levi, R., Karube, I., & Wulff, G. (1998). Imprinted membranes for sensor technology: opposite behavior of covalently and noncovalently imprinted membranes. *Macromolecules*, *31*(7). https://doi.org/10.1021/ma970818d

Piletsky, S., & Turner, A. (2004). A New Generation of Chemical Sensors Based on MIPs. In *Molecular Imprinting of Polymers*.

Plata-Nazar, K., & Jankowska, A. (2011). Clinical usefulness of determining the concentration of Neopterin. *Pteridines*, *22*(3), 77–89. https://doi.org/10.1515/PTERIDINES.2011.22.1.77

Prabowo, B. A., Wang, R. Y. L., Secario, M. K., Ou, P. T., Alom, A., Liu, J. J., & Liu, K. C. (2017). Rapid detection and quantification of Enterovirus 71 by a portable surface plasmon resonance biosensor. *Biosensors & Bioelectronics*, *92*, 186–191. https://doi.org/10.1016/J.BIOS.2017.01.043

Puiu, M., & Bala, C. (2016a). SPR and SPR Imaging: Recent Trends in Developing Nanodevices for Detection and Real-Time Monitoring of Biomolecular Events. *Sensors (Basel, Switzerland)*, *16*(6). https://doi.org/10.3390/S16060870

Rayleigh, Lord. (1907). On the dynamical theory of gratings. *Proceedings of the Royal Society of London. Series A, Containing Papers of a Mathematical and Physical Character*, *79*(532), 399–416. https://doi.org/10.1098/RSPA.1907.0051

Razumovitch, J. A., Semenkova, G. N., Fuchs, D., & Cherenkevich, S. N. (2003). Influence of Neopterin on the generation of reactive oxygen species in human neutrophils. *FEBS Letters*, *549*(1–3), 83–86. https://doi.org/10.1016/S0014-5793(03)00796-8

Sakurai, A., & Goto, M. (1967). Neopterin: Isolation from human urine. In *Journal of Biochemistry* (Vol. 61, Issue 1). https://doi.org/10.1093/oxfordjournals.jbchem.a128513

Say, R., Birlik, E., Ersöz, A., Yilmaz, F., Gedikbey, T., & Denizli, A. (2003). Preconcentration of copper on ion-selective imprinted polymer microbeads. *Analytica Chimica Acta*, *480*(2), 251–258. https://doi.org/10.1016/S0003-2670(02)01656-2

Scarano, S., Mascini, M., Turner, A. P. F., & Minunni, M. (2010). Surface plasmon resonance imaging for affinity-based biosensors. *Biosensors & Bioelectronics*, *25*(5), 957–966. https://doi.org/10.1016/J.BIOS.2009.08.039

Schasfoort, R. B. M., & McWhirter, A. (2008). Chapter 3:SPR Instrumentation. *Handbook of Surface Plasmon Resonance*, 35–80. https://doi.org/10.1039/9781847558220-00035

Sharma, P. S., Wojnarowicz, A., Sosnowska, M., Benincori, T., Noworyta, K., D'Souza, F., & Kutner, W. (2016). Potentiometric chemosensor for Neopterin, a cancer biomarker, using an electrochemically synthesized molecularly imprinted polymer as the recognition unit. *Biosensors & Bioelectronics*, *77*, 565–572. https://doi.org/10.1016/J.BIOS.2015.10.013

Shea, K. J., & Dougherty, T. K. (2002). Molecular recognition on synthetic amorphous surfaces. The influence of functional group positioning on the effectiveness of molecular recognition. *Journal of the American Chemical Society*, *108*(5), 1091–1093. https://doi.org/10.1021/JA00265A046

Shi, L., Sun, Q., He, an, Xu, H., Liu, C., Zhao, C., Xu, Y., Wu, C., Xiang, J., Gu, D., Long, J., & Lan, H. (2015). *Development of SPR biosensor for simultaneous detection of multiplex respiratory viruses 1*. https://doi.org/10.3233/BME-151526

Sucher, R., Schroecksnadel, K., Weiss, G., Margreiter, R., Fuchs, D., & Brandacher, G. (2010). Neopterin, a prognostic marker in human malignancies. In *Cancer Letters* (Vol. 287, Issue 1). https://doi.org/10.1016/j.canlet.2009.05.008

Tomandl, J., Tallova, J., Tomandlova, M., & Palyza, V. (2003). Determination of total oncopterin, Neopterin and biopterin in human urine by high performance liquid chromatography with solid phase extraction. *Journal of Separation Science*, *26*(8). https://doi.org/10.1002/jssc.200301371

Turgan, N., Habif, S., Parildar, Z., Özmen, D., Mutaf, I., Erdener, D., & Bayindir, O. (2001). Association between homocysteine and Neopterin in healthy subjects measured by a simple HPLC-fluorometric method. *Clinical Biochemistry*, *34*(4). https://doi.org/10.1016/S0009-9120(01)00226-0

Victoria, S. (2012). Application of Surface Plasmon Resonance (SPR) for the Detection of Single Viruses and Single Biological Nano-objects. *Journal of Bacteriology & Parasitology*, *03*(07). https://doi.org/10.4172/2155-9597.1000E110

Vrecko, K., Staedtler, P., Mischak, I., Maresch, L., & Reibnegger, G. (1997). Periodontitis and concentrations of the cellular immune activation marker Neopterin in saliva and urine. *Clinica Chimica Acta; International Journal of Clinical Chemistry*, *268*(1–2), 31–40. https://doi.org/10.1016/S0009-8981(97)00154-X

Wachter, H., Fuchs, D., Hausen, A., Reibnegger, G., & Werner, E. R. (1989). Neopterin as marker for activation of cellular immunity: immunologic basis and clinical application. *Advances in Clinical Chemistry*, *27*(C), 81–141. https://doi.org/10.1016/S0065-2423(08)60182-1

Wachter, H., Hausen, A., & Grassmayr, K. (1979). Erhohte Ausscheidung Von Neopterin Im Harn Vom Patienten Mit Malignen Tumoren Und Mit Viruserkrankungen. *Hoppe-Seyler's Zeitschrift Fur Physiologische Chemie*, *360*(12).

Wackerlig, J., & Lieberzeit, P. A. (2015). Molecularly imprinted polymer nanoparticles in chemical sensing - Synthesis, characterisation and application. In *Sensors and Actuators, B: Chemical* (Vol. 207, Issue Part A). https://doi.org/10.1016/j.snb.2014.09.094

Wei, S., Jakusch, M., & Mizaikoff, B. (2006). Capturing molecules with templated materials--analysis and rational design of molecularly imprinted polymers. *Analytica Chimica Acta*, *578*(1), 50–58. https://doi.org/10.1016/J.ACA.2006.06.077

Werner, E. R., Werner-Felmayer, G., Fuchs, D., Hausen, A., Reibnegger, R., Yim, J. J., & Wachter, H. (1991). Biochemistry and function of pteridine synthesis in human and murine macrophages. *Pathobiology : Journal of Immunopathology, Molecular and Cellular Biology*, *59*(4), 276–279. https://doi.org/10.1159/000163662

Westermann, J., Thiemann, F., Gerstner, L., Tatzber, F., Kozák, I., Bertsch, T., & Krüger, C. (2000). Evaluation of a new simple and rapid enzyme-linked immunosorbent assay kit for Neopterin determination. *Clinical Chemistry and Laboratory Medicine*, *38*(4). https://doi.org/10.1515/CCLM.2000.050

Widner, B., Baier-Bitterlich, G., Wede, I., Wirleitner, B., Wachter, H., & Fuchs, D. (1998). Neopterin: Indicator of oxidative stress and part of the cytotoxic armature of activated macrophages in humans. *Pteridines*, *9*(2), 91–102. https://doi.org/10.1515/PTERIDINES.1998.9.2.91/MACHINEREADABLECITATION/RIS

Widner, B., Laich, A., Sperner-Unterweger, B., Ledochowski, M., & Fuchs, D. (2002). Neopterin production, tryptophan degradation, and mental depression--what is the link? *Brain, Behavior, and Immunity*, *16*(5), 590–595. https://doi.org/10.1016/S0889-1591(02)00006-5

Widner, B., Wirleitner, B., Baier-Bitterlich, G., Weiss, G., & Fuchs, D. (2000). Cellular immune activation, Neopterin production, tryptophan degradation and the development of immunodeficiency. *Cellular Immune Activation, Neopterin Production, Tryptophan Degradation and the Development of Immunodeficiency*, *48*(4), 251–258. https://pubmed.ncbi.nlm.nih.gov/11059641/

William, J., Saad, N., Salib, M., Riad, H., Mahran, K. S., Iskander, I., Cozma, G., & Barsoum, R. (1998). The acute effect of intravenously administered recombinant human erythropoietin on the immune response of uremic patients maintained on regular hemodialysis. *Artificial Organs*, *22*(3), 192–196. https://doi.org/10.1046/J.1525-1594.1998.06041.X

Wirleitner, B., Obermoser, G., Böck, G., Neurauter, G., Schennach, H., Sepp, N., & Fuchs, D. (2003). Induction of apoptosis in human blood T cells by 7,8-dihydroNeopterin: The difference between healthy controls and patients with systemic lupus erythematosus. *Clinical Immunology*, *107*(3). https://doi.org/10.1016/S1521-6616(03)00040-8

Włoch, M., & Datta, J. (2019). Synthesis and polymerisation techniques of molecularly imprinted polymers. *Comprehensive Analytical Chemistry*, *86*, 17–40. https://doi.org/10.1016/BS.COAC.2019.05.011

Wood, R. W. (2009). XLII. On a remarkable case of uneven distribution of light in a diffraction grating spectrum. *Https://Doi.Org/10.1080/14786440209462857*, *4*(21), 396–402. https://doi.org/10.1080/14786440209462857

Wood, R. W. (2010). XXVII. Diffraction gratings with controlled groove form and abnormal distribution of intensity. *Https://Doi.Org/10.1080/14786440208637224*, *23*(134), 310–317. https://doi.org/10.1080/14786440208637224

Wulff, G., & Knorr, K. (2001). Stoichiometric noncovalent interaction in molecular imprinting. *Bioseparation 2001 10:6*, *10*(6), 257–276. https://doi.org/10.1023/A:1021585518592

Wulff, G., Vietmeier, J., & Poll, H.-G. (1987). Enzyme-analogue built polymers, 22. Influence of the nature of the crosslinking agent on the performance of imprinted polymers in racemic resolution. *Die Makromolekulare Chemie*, *188*(4), 731–740. https://doi.org/10.1002/MACP.1987.021880407

Yan, H., & Kyung, H. R. (2006). Characteristic and synthetic approach of molecularly imprinted polymer. *International Journal of Molecular Sciences*, *7*(5–6), 155–178. https://doi.org/10.3390/I7050155

Yan, M., & Ramström, Olof. (2005). *Molecularly imprinted materials : science and technology*. 734.

Yavuz, H., Say, R., & Denizli, A. (2005). Iron removal from human plasma based on molecular recognition using imprinted beads. *Materials Science and Engineering: C*, *25*(4), 521–528. https://doi.org/10.1016/J.MSEC.2005.04.005

Yola, M. L., Atar, N., & Eren, T. (2014). Determination of amikacin in human plasma by molecular imprinted SPR nanosensor. Sensors and Actuators B: Chemical, 198, 70-76.

Zhang, H., Ye, L., & Mosbach, K. (2006). Non-covalent molecular imprinting with emphasis on its application in separation and drug development. *Journal of Molecular Recognition*, *19*(4), 248–259. https://doi.org/10.1002/JMR.793

Zhang, J., Zhu, J., Feng, Y., Hu, D., Lv, H., Zhu, J., Cao, M., Zheng, F., Gong, X., Hao, L., Srinivas, S., Ren, H., Qi, Z., Li, B., & Wang, C. (2013). Rapid and sensitive detection of H7N9 avian influenza virus by use of reverse transcription-loop-mediated isothermal amplification. *Journal of Clinical Microbiology*, *51*(11), 3760–3764. https://doi.org/10.1128/JCM.01907-13

Zhang, Z., Ma, X., Li, B., Zhao, J., Qi, J., Hao, G., Jianhui, R., & Yang, X. (2020). Fluorescence detection of 2,4-dichlorophenoxyacetic acid by ratiometric fluorescence imaging on paper-based microfluidic chips. *Analyst*, *145*(3), 963–974. https://doi.org/10.1039/C9AN01798D

Zimmerman, A. W., Jyonouchi, H., Comi, A. M., Connors, S. L., Milstien, S., Varsou, A., & Heyes, M. P. (2005). Cerebrospinal fluid and serum markers of inflammation in autism. *Pediatric Neurology*, *33*(3). https://doi.org/10.1016/j.pediatrneurol.2005.03.014

Zvetkova, E., Wirleitner, B., Tram, N. T., Schennach, H., & Fuchs, D. (2001). Aqueous extracts of Crinum latifolium (L.) and Camellia sinensis show immunomodulatory properties in human peripheral blood mononuclear cells. *International Immunopharmacology*, *1*(12). https://doi.org/10.1016/S1567-5769(01)00140-0

Zybin, A., Kuritsyn, Y. A., Gurevich, E. L., Temchura, V. v., Überla, K., & Niemax, K. (2010). Real-time detection of single immobilized nanoparticles by surface plasmon resonance imaging. *Plasmonics*, *5*(1), 31–35. https://doi.org/10.1007/S11468-009-9111-5/FIGURES/4